

Chapter 13

Flood Risk Assessment and Numerical Modelling of Flood Simulation in the Damodar River Basin, Eastern India



Sandipan Ghosh  and Soumya Kundu

Abstract In the Damodar River Basin, the streamflow is scientifically controlled and regulated by the five large dams (viz., Panchet, Maithon, Konar, Tilaiya, and Tenughat) since the 1950s to manage irrigation water and floods in West Bengal, but currently, the water holding capacity of Damodar River and DVC (Damodar Valley Corporation) reservoirs (including Durgapur Barrage) is reduced due to siltation and lack of maintenance. For that reason, the recurrent flood events of each year, with minimum critical discharge of $1651\text{--}1822\text{ m}^3\text{s}^{-1}$, are triggered in the low-lying floodplains of Purba Bardhaman, Hooghly, and Howrah districts. The channels of lower Damodar basin (viz., Mundeswari and Damodar/Amta) are supposed to drain $7079\text{ m}^3\text{s}^{-1}$ of water, but these are actually able to handle only $2832\text{ m}^3\text{s}^{-1}$ of water during monsoon months. Nowadays, the government officials of West Bengal have blamed the flood regulation system of DVC, and they characterized this flood phenomenon as “man-made hazard.” Using advanced geospatial techniques, the present study tries to encompass the key factors of hydrometeorological floods and contemporary flood dynamics in the lower Damodar River Basin (Damodar fan-delta region of West Bengal), viz., analysis of flood-generated rainfall events, rainfall–runoff simulation, prediction of probable maximum flood, dam-included changes in flood hydrology, and 1D hydrodynamic flood model of steady and unsteady flow.

Keywords Flood frequency analysis · Curve number · 1D hydrodynamic model · Mann-Kendall test · Damodar River Basin · HEC-RAS

1 Introduction

Flood risk assessment (FRA) integrates two distinct parts: (a) estimating flood probability of certain return periods and the flood discharge of particular magnitude and (b) assessing the variable dimensions of flood risk, hydrogeomorphic

S. Ghosh (✉) · S. Kundu

Department of Geography, Chandrapur College, Purba Bardhaman, West Bengal, India

mechanisms of floods, flood controlling strategies, and real-time actions to be taken before during the floods (Hall & Penning-Rosewell, 2011). Floods are basically extreme hydrological phenomena, and it, generated by natural and anthropogenic causes, represents a classic example of the “pulsed type of disturbance” in the fluvial system (Kington, 2014). The term “flood” has a range of meanings, including (1) hydrological floods with different magnitude and inconstant flow frequency in connection with climate change; (2) floods as hazard and vulnerability, damaging, and livelihoods; and (3) consequences of floods on the components of environment and landscape change (Baker, 1994). A flood event may occur due to large streamflow magnitude as such as that the flow rate exceeds the capacity of the main channel at a location (i.e., the flow exceeds the bankfull discharge) or may occur for a lower streamflow rate when the flow happens at a time when the channel is fully or partially obstructed, as can occur with ice jam or as a result of debris flow in the channel (Burn et al., 2017). The floods of Indian rivers are very important hydrogeomorphic hazard, and the monsoon floods are inevitable and recurrence event because flooding is the natural mechanism (intensified by human activities) by which excess runoff water is discharged through channels, and occasionally it overflows in the floodplains (Kale, 2003; Sinha et al., 2012). In West Bengal, floods are natural as well as man-made hazards which cause considerable damages, particularly in the populated areas of lower Damodar River Basin. The main concern is economic impacts of floods (triggering poverty at village level) including costs due to loss of, or damage to, property, infrastructure damage or destruction, loss of crops and livestock, and lost wages and productivity due to more disruptions.

The flood account of Damodar River, hydrometeorology, nature of annual monsoon floods, structural measures of flood mitigation, changing flood dynamics and floodplain morphology, fluvial aggradation and degradation, dam-controlled environmental flow, role of human on flood hydrology and geomorphology, and impact of flood in agrarian society were previously studied and discussed in details by Glass (1924), Kirk (1950), Pramanik and Rao (1952), Bagchi (1977), Saha (1979), Sen (1985), Roy and Mazumdar (2007), Majumder et al. (2010a), Bhattacharya (2011), Ghosh (2011), Choudhury (2012), Lahiri-Dutt (2012), Lahiri-Dutt and Samanta (2013), Bera and Mistri (2014), Rajbanshi (2015), Ghosh and Mistri (2015), Ghosh and Guchhait (2016), Verma et al. (2017), Das et al. (2017), Chattopadhyay et al. (2020), Mahata and Maiti (2020), Ghosh and Illahi (2020), Ghosh et al. (2021, 2022a), and Hoque et al. (2022). Before dam construction, the floods were very violent in nature (exceeding $18,000 \text{ m}^3 \text{ s}^{-1}$ peak flow) and devastating in this funnel-shaped basin, damaging economic assets and livelihood to a large extent, and it was renowned as the “Sorrow of Bengal.” In the 1950s, the DVC (Damodar Valley Corporation) had been introduced the first multipurpose river valley project of India to boost up the regional economy of eastern India and to manage annual flood peaks. Carrying more than 75 years of legacy the DVC has partly achieved the objectives of planning, but the lower segment of the Damodar River (two bifurcated branches – Mundaswari and Damodar/Amta channel) is still vulnerable to recurrent flood hazard during peak monsoon rainfall or tropical depression. At present, elevated embankments and large dams have progressively altered the morphology and

hydrology of the fluvial system to a great extent, and the problems of ecological degradation, water pollution, water security, downstream flood hazard, reservoir siltation, drainage congestion, degradation of palaeochannels or spill channels (i.e., floodways of fan-delta), and declining carrying capacity of channel (accommodating diminutive bankfull discharge) are the key issues.

The assessment of flood hydrological dynamics and risk is an essential part of water resource management, especially in a dam-controlled river. Flood forecasting model, a tool of FRA, only makes sense if its results reach as many of the affected people as possible in a suitable form (Sharma et al., 2022). At present, the application of flood and river analysis software and machine learning process in the field of flood hydrology and river flow simulation/hydrodynamic model is a popular practice to develop better flood management at spatial scale (Correia et al., 1998; Leandro et al., 2009; Albano et al., 2017; Mojaddadi et al., 2017; Teng et al., 2017; Sharma et al., 2022). The HEC-RAS (Hydrologic Engineering Center's River Analysis System) developed by the US Army Corps of Engineers is a toolkit (an open-source software, <https://www.hec.usace.army.mil/software/hecras/>) of hydrologists and river scientists that allows the user to perform one-dimensional steady flow, one- and two-dimensional unsteady flow calculations, sediment transport/mobile bed computations, and water temperature/water quality modelling (Goodarzi & Eslamain, 2022). The application of HEC-RAS software for flood simulation and floodplain inundation was successfully executed by Horritt and Bates (2002), Merwade et al. (2008), Gibson et al. (2010), Pender and Neelz (2011), Sarhadi et al. (2012), Khattak et al. (2016), Dasallas et al. (2019), Kumar et al. (2019), Farooq et al. (2019), Ongdas et al. (2020), Pathan and Agnihotri (2020), Mawasha (2021), and Rana and Suryanarayana (2021). In numerous studies, HEC-RAS one-dimensional (1D) or two-dimensional (2D) hydrodynamic models are used to simulate flood flows, environmental flows, spatial coverage of floodplain inundation, flood depth, sediment transport along channel, flow velocity in respect of variable discharge, culvert flow design, spatial variability of water quality, and scour phenomenon at bridge piers (Tate & Maidment, 1999; Goodell, 2005; Knebl et al., 2005; Lee et al., 2006; Parsa et al., 2013; Mawasha, 2021). Alongside the floods of Indian rivers (viz., Krishna, Yamuna, Teesta, Mahanadi, Dwarkeswar, Bhagirathi-Hooghly etc.) and unsteady flow simulation were assessed using the hydrodynamic models of HEC-RAS (Mandal & Chakrabarty, 2016; Kumar et al., 2017; Patel et al., 2017; Surwase et al., 2020; Pathan & Agnihotri, 2020; Jagadesh & Veni, 2021; Malik & Pal, 2021; Rana & Suryanarayana, 2021; Ghosh et al., 2022b). It is essential to mention that in the Damodar River the hydraulic routing of extreme floods, 1D/2D flood simulation, 1D-2D coupled LISFLOOD-FP model, and TELEMAC-2D model were analyzed by Sanyal et al. (2013, 2014a, b), Sanyal (2017), and Singh et al. (2020, 2021).

These studies already show that the HEC-RAS software makes it possible to determine how high the water surface will be in the floodplain during specific discharge and which areas are affected by it (Goodarzi & Eslamain, 2022). The study of an inundation area (an area of land subject to flooding) and the evaluation of its water surface level are the most important part of each flood risk management

project (Ogras & Onen, 2020). For floodplain modelling and visualization of input or output data, HEC-RAS is designed in order to model the hydrologic engineering properties of river flow and to import/export data to ArcGIS platform to facilitate the decision-making (Ogras & Onen, 2020). To improve the flood management system of riparian terrain, the utmost vital tool of HEC-RAS software is to check the magnitude of flood risk and vulnerability of flood-prone region, determining the critical floodplain boundaries of maximum flood flow. As the river floodplain zoning maps provide valuable hydrologic information, such as flow area, frictional loss, Froude number, hydraulic conveyance, critical hydraulic depth, flood depth, and area of flood prevention in flood zones, it is decisive to place the maps in the first step of flood management (ShahiriParsa et al., 2016). Observing the potentiality of HEC-RAS, the present study aims to assess the dam-induced changes in the occurrence of extreme floods, floodplain inundation during unsteady flows, and the associated floodplain risk of variable return period discharge (2-year, 5-year, 10-year, 25-year, 50-year, and 100-year floods) in the lower part of Damodar River Basin. Heavy rainstorm event of monsoon climate, runoff yield of different terrain (hard rock or alluvium), and flash floods have inevitable in situ uncertainty with a physical open system, but if the current estimates of flood flow or bankfull discharge or carrying capacity of Damodar River can be deduced, then an idea of flood risk can be derived with some statistical perception.

2 Geographical Settings of Study Area

The Damodar River Basin (DRB) covers a basin area of 23,370 km² in Jharkhand and West Bengal. Its latitudinal extension ranges from 23° to 23° 22' 10" N, and the longitudinal extension ranges from 87°28'23" to 88°01'00" E. The 541-km-long stretch of Damodar starts its journey from the Khamarpat Hill (altitude 1062 m from mean sea level) of Chandwa, Palamu district (Jharkhand). The main tributaries of upper catchment are Barakar, Konar, Gobai, Jamuniya, Haharo, Garhi, Bhera, and Uttala. Below the Durgapur Barrage, the River receives the last tributary, named Sali. Following almost linear channel pattern (eastern ward slope), the river takes a sharp 90 southward turn at Palla (24 km east of Bardhaman town). At Paikpara, Jamalpur the main river bifurcates into two distributaries (Mundeswari at west and Damodar/Amta channel at east), and the Amta channel joins the Bhagirathi-Hooghly River at Falta, Howrah (48.3 km south of Kolkata). From the elbow of 90 turn several spill channels and palaeochannels (old distributaries of Damodar) are observed showing the topographic signature of fan-delta formation (prograding towards east and southeast direction) and palaeofloodways of monsoon months. Below the bifurcation point both channels, Mundeswari and Damodar/Amta channel, is confined within embankments, but bankfull discharge and monsoonal overflow make this floodplain or active fan-delta a flood-prone region of West Bengal which includes agriculturally dominated blocks of Pursura, Tarakeswar, Khanakul I and II, Jangipara, Udaynarayanpur, and Amta I and II. The main hydrologic concern

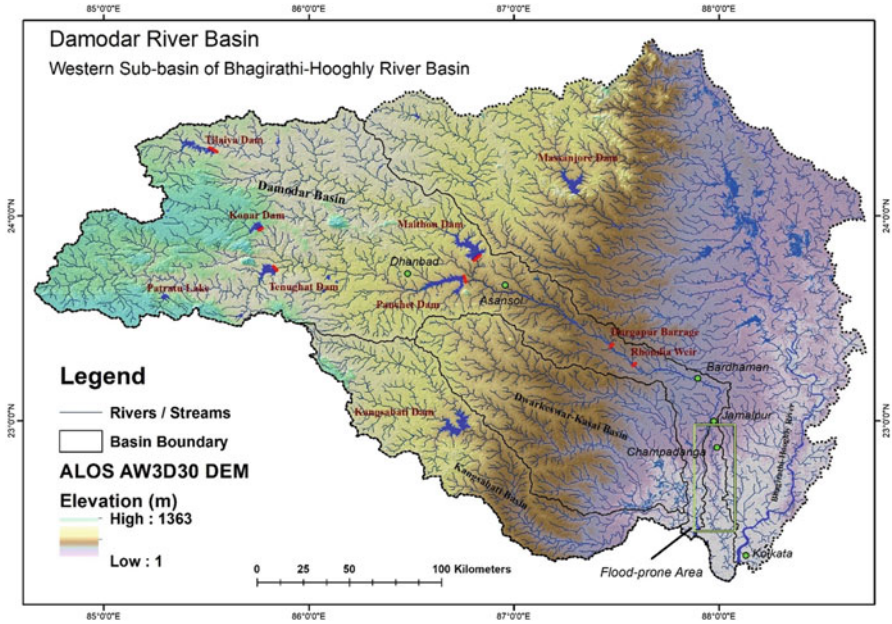


Fig. 13.1 Location map of Damodar River Basin (including sites of dams, barrage, and weir) on ALOS AW3D30 DEM, along with associated western sub-basins of Bhagirathi-Hooghly River System

is the lower fluvial system of Damodar River which extends from $22^{\circ} 35' 42''$ to $23^{\circ} 09' 30''$ N and $87^{\circ} 51' 08''$ to $88^{\circ} 00' 31''$ E.

The DRB (Fig. 13.1) is located in the topographic transitional zone (break of slope) of the Chhotanagpur Plateau (west) and the Bengal Basin (east), following three major south-north trend basement faults – (1) Chhotanagpur Foothill fault, (2) Pingla Fault, and (3) Khandagosh-Garhmayna fault (Ghosh & Guchhait, 2015; Mahata & Maiti, 2019). In the upper part of Damodar, the slope is 1.86 m km^{-1} for the first 241 km, and for the next 167 km, it is 0.57 m km^{-1} , and in the lower part, it is only 0.16 m km^{-1} (Mahata & Maiti, 2019). The upper part of the basin (upstream of Durgapur) is covered mainly by granite and gneiss of the Archean, Gondwana sandstone and shale, and Recent channel alluvium, whereas the lower part (downstream of Durgapur) is characterized by the deposits of tertiary sediments, Early-Late Pleistocene laterites and Late Pleistocene – Recent alluvium (Mahata & Maiti, 2019). Since Oligocene (34–23 Ma BP), influenced by several marine transgression and regression periods, the vast load of plateau sediments was deposited by the fluvial system of Damodar, and it filled up the western shelf zone of the Bengal Basin in the subaerial and subaqueous tropical palaeoenvironment (Mahata & Maiti, 2019). By process of avulsing channels, sheet flow and debris flow the total fan-delta of Damodar (below Panagrah, Paschim Bardhaman) prograded into the shallow marine condition of the Bengal Basin. Downstream of Panagrah, the topography of lower Damodar River is subdivided into three distinct fan-deltaic

parts – (1) Early Pleistocene to Late Pleistocene Panagarh fan-delta (trending east), (2) Late Pleistocene to Early Holocene Memari fan-delta (trending southeast), and (3) Late Holocene to Recent active fan-delta (trending south) (Acharyya & Shah, 2007; Mahata & Maiti, 2019) (Fig. 13.1).

The most significant part of the basin is large-scale modification of channels by installing large dams, and to understand the anthropogenic impact on fluvial system, the DRB is a practical example from India. Perceived in 1945, following the model of the Tennessee Valley Authority (TVA), the Damodar Valley Corporation (DVC) was designed in 1948 under the guidance of Dr. Meghnad Saha and W.L. Voorduin who had been provided the total framework of multipurpose Damodar Valley Project, named “Preliminary Memorandum on the Unified Development of the Damodar River.” DVC was aimed to integrate the people, water, cropland, and mineral resources in a single thread of sustainable development with a holistic approach (Kirk, 1950; Saha, 1979). Firstly, it was decided to build eight large dams at eight sites, viz., (1) Tilaiya, Maithon, and Balpahari dams on the Barakar River; (2) Bokaro dam on Bokaro River; (3) Konar on Konar River; and (4) Aiyer, Bermo, and Panchet on Damodar River (Chandra, 2003). Finally, DVC decided to build only four dams at first phase, viz., Tilaiya (1953), Konar (1955), Maithon (1957), and Panchet (1959) (Table 13.1). After that, in 1974 one more reservoir, Tenughat, on the Damodar River was built. The Durgapur Barrage, built in 1955, is one of the important river impoundments because it finally releases incoming excess runoff water which has potentiality to flood in the lower floodplain of Damodar. Eight large dams would be able to reduce peak discharge of $28,321 \text{ m}^3 \text{ s}^{-1}$ (resulting from a rainstorm of 50.8 cm at the upper catchment) to $7080 \text{ m}^3 \text{ s}^{-1}$ at Rhondia, having total flood reserve of 6500 million m^3 , but five dams only provide a maximum storage capacity of 3591 million m^3 (Bhattacharya, 2011). Now DVC flood-controlling system provides a flood benefit of only 162.56 mm of surface runoff to the lower part of the basin, in place of 452 mm as advocated by the committee (Ghosh & Guchhait, 2016). Living on the active floodplain of Damodar and its structural modifications for protection against floods and for utilization of regional resources and wealth has aggravated the problem of hydrological risk factor to inundation (Table 13.1).

3 Methodology

The present study incorporates selected quantitative methods and techniques used in flood hydrology which deals with hydrometeorological aspects of flood, alluvial channel dynamics, flood routing and flood stage identification, hydraulic and engineering dimensions of floods, holistic flood risk assessment, and integrated flood management. Alongside, the methods of fluvial hydrology (Ward, 1978; Garde, 2006) include estimation of channel planforms and geometric dimensions (viz., width, depth, slope, sinuosity, sediment, channel roughness, etc.) and river hydraulics (viz., flow pattern, regime, hydrograph, and discharge anomalies). Along with

Table 13.1 Overview and salient features of the dams in the Damodar River Basin

Dams/barrage River	Tenughat Damodar	Konar	Tilaiya Barakar	Maithon Barakar	Panchet Damodar	Durgapur Barrage
Inauguration year	1974	1955	1953	1957	1959	1955
Location	23°44' N 85°55' E	23°43' N 85°30' E	24°19' N 85°31' E	23°78' N 86°81' E	23°40' N 86°44' E	24°06' N 86°13' E
Catchment area (km ²)	3393	997	984	6293	10,966	19,555
Dam height (m)	55.0	57.6	30.18	56.08	47.85	—
Annual runoff (m ³)	2,450,000,000	555,070,000	431,720,000	2,614,990,000	4,539,230,000	—
Total dead storage (m ³)	160,960,000	34,400,000	74,780,000	93,170,000	119,140,000	—
Spillway design discharge (m ³ s ⁻¹)	15,990	6796	1348	13,592	16,608	—
Minimum annual flow (m ³ s ⁻¹)	69.83	13.63	10.37	81.5	135.87	168.03
Environmental flow (m ³ s ⁻¹) Q50 7-days	39.17	22.59	22.05	62.88	71.25	193.81

Source: Verma et al. (2015)

the techniques of flood prediction and modelling, the aim of flood hydrologic assessment is providing assistance and preliminary information to manage active floodplain zones and vulnerable flooded areas with the help of 1D or 2D hydrodynamic model and advanced geo-spatial tools.

3.1 Data Collection

The primary spatial information of study area was mostly collected from the topographical sheets (73 M/7, M/11, M/12, M/15, M/16, N/13, and 19 A/4) of SOI (Survey of India). The topographic and hydrological information of DRB were collected from the book, entitled “The Planning Atlas of the Damodar Valley Region,” which was written by Chatterjee (1969). The up-to-date daily rainfall, gauge data, and reservoir discharge data were retrieved from the official website (<https://www.wbiwd.gov.in/>) of IWD (Irrigation and Waterways Department, Government of West Bengal). In this study the main river gauge data (gauge level in metre) was collected for the four IWD monitoring stations – (1) Rhondia (23° 22' 56" N, 87° 29' 35" E), (2) Edilpur (23° 13' 40" N, 87° 49' 12" E), (3) Jamalpur (23° 02' 39" N, 87° 58' 56" E), (4) Champadanga (22° 50' 24" N, 87° 58' 12" E), and (5) Harinkhola (22° 50' 22" N, 87° 54' 16" E) (Fig. 13.2). The daily IWD reservoir discharge data were collected for the Durgapur Barrage (23° 38' 35" N, 87° 18' 11" E). The historical flood data and annual peak flow data of the DRB were collected from the research paper of Glass (1924), annual flood report of IWD (1959 and 2000), the books of Bhattacharya (2011) and Rudra (2018), and the research papers of Das et al. (2017) and Majumder et al. (2010b). The basin map of Damodar was prepared from the data repository of HydroSHEDS (Hydrological data and maps based on Shuttle Elevation Derivating at multiple scale). HydroRIVERS has been extracted from the gridded HydroSHEDS core layers at 15 arc-second resolution. The surface geology, lineaments, drainage, and other geomorphic information and thematic maps were retrieved from the web portal of the Geological Survey of India (www.bhukosh.gsi.gov.in). Monthly and annual rainfall data were retrieved from the CHRS (Center for Hydrometeorology and Remote Sensing) data portal (www.chrs.eng.uci.edu) which provided gridded precipitation data of resolution $0.04^\circ \times 0.04^\circ$ (4×4 km). The rainfall data belongs to PERSIANN (Precipitation Estimation from Remotely Sensed Information using Artificial Neural Networks) CCS (Cloud Classification System) algorithm, which relates to variable threshold cloud segmentation (Nguyen et al., 2019). Alongside, another $0.25^\circ \times 0.25^\circ$ resolution gridded rainfall data was collected from the official website of the Indian Meteorological Department (www.imdpune.gov.in). The land use and land cover (LULC) information were collected from the web portal of ESRI 2020 Land Cover Downloader (<https://www.arcgis.com/home/item.html?id=fc92d38533d440078f17678ebc20e8e2#overview>) where the analysis was done using the Sentinel – 10 m resolution imagery (2017–2021). The ALOS Global Digital Surface Model (AW3D30) digital elevation data of 30 m resolution was collected from the web portal of Open Topography. The

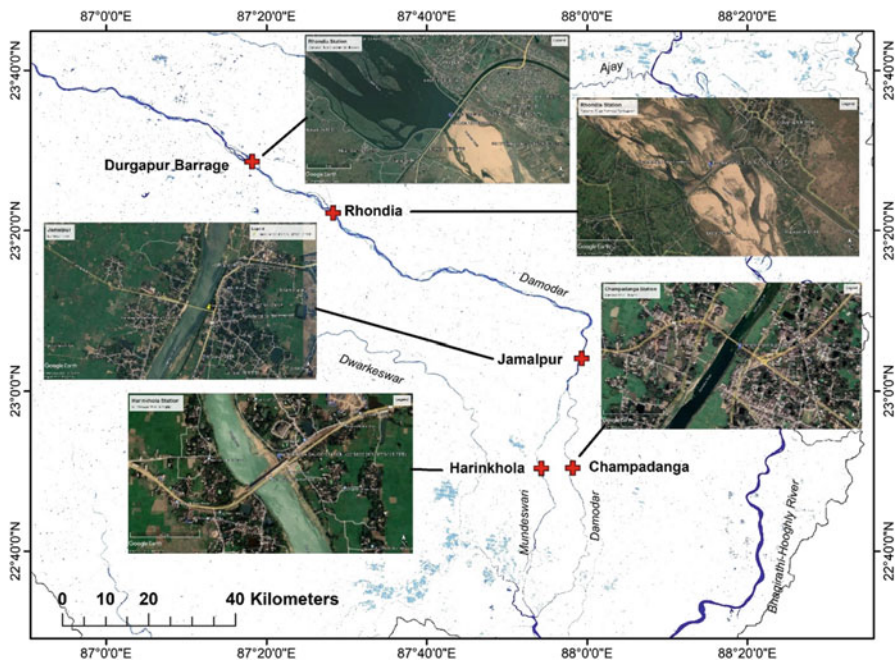


Fig. 13.2 Important sites of river gauge stations and Durgapur Barrage in the lower Damodar River Basin (West Bengal)

Japan Aerospace Exploration Agency (JAXA) releases the global digital surface model (DSM) dataset of AW3D30 with a horizontal resolution of 30-meter mesh (1 arcsec). The dataset of surface water occurrence (SWO) was gathered from the web portal (www.global-surface-water.appspot.com/download) of the Joint Research Centre's Global Surface Water Dataset (1984–2020) which was prepared to analyse the seasonal occurrence of inundated areas and permanent water bodies. National level hydrological modelling framework (National Remote Sensing Centre, Hyderabad) provides the database of evapotranspiration, surface runoff, and soil moisture on a daily basin of 5.5 km grid resolution in India (www.bhuvan.nrsc.gov.in/nhp). In this study, all databases are analysed and spatially mapped in the ERDAS Imagine 2014, ArcGIS 10.4, HEC-RAS 6.2, and XLSTAT (Table 13.2).

4 Methods

4.1 Basics of 1D-Hydrodynamic Model

One-dimensional (1D) hydrodynamic model in flood simulation assumes that the phenomenon of peak streamflow can be defined satisfactorily as unsteady or steady

Table 13.2 Important sources of secondary database

Sl. no.	Data	Provider	Web portal
1	Daily rainfall, gauge data, and reservoir discharge	Irrigation and Waterways Department, Government of West Bengal	www.wbiwd.gov.in/
2	Hydrological data and maps	HydroSHEDS	www.hydrosheds.org/page/hydrobasins
3	Surface geology, lineaments, drainage, and other geomorphic information	Geological Survey of India	www.bhukosh.gsi.gov.in
4	Monthly and annual rainfall data	Center for Hydrometeorology and Remote Sensing	www.chrs.eng.uci.edu
5	Land use and land cover	Environmental Systems Research Institute	https://www.arcgis.com/home/item.html?id=fc92d38533d440078f17678ebc20e8e2#overview
6	Digital elevation model data	Japan Aerospace Exploration Agency	https://portal.opentopography.org/raster?opentopoID=OTALOS.112016.4326.2
7	Dataset of surface water occurrence	Joint Research Centre's Global Surface Water Dataset	www.global-surface-water.appspot.com/download
8	Global hydrologic soil groups database	National Aeronautics and Space Administration	https://catalog.data.gov/dataset/global-hydrologic-soil-groups-hysogs250m-for-curve-number-based-runoff-modeling
9	Database of evapotranspiration, surface runoff, soil moisture	National Remote Sensing Centre	www.bhuvan.nrsc.gov.in/nhp

flow (with certain geometry and boundary conditions of channel) in a space of single dimension. 1D flood model was elaborated and applied by numerous workers (Horritt & Bates, 2002; Merwade et al., 2008; Leondro et al., 2009; Pender & Neelz, 2011; Betsholtz & Nordlof, 2017; Dasallas et al., 2019). 1D- hydrodynamic model is based on the Bernoulli (energy equation) and Saint-Venant equations (mass and moment conservation) for steady and unsteady flows in open channels, respectively. Betsholtz and Nordlof (2017) mentioned the following assumptions behind 1D flood simulation:

- The fluid is incompressible. Where the density of fluid is constant, the volume should be proportional to the mass.
- It is assumed that the water flows follow a longitudinal direction.
- In pressure distribution along a channel, the hydrostatic and vertical accelerations are overlooked.
- Vertical variations in flow and velocity are ignored.
- The water depth is much lower than the wave lengths.
- The average channel bed slope is small.

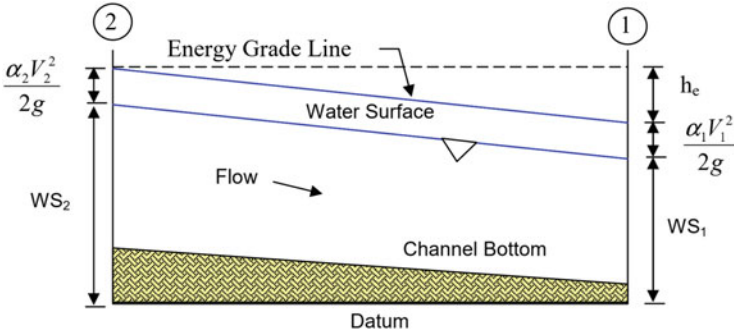


Fig. 13.3 A schematic diagram of 1D hydrodynamic model (where α_1 and α_2 = velocity weighting coefficients; V_1 and V_2 = average velocity; g = gravitational acceleration; h_e = energy head loss; WS_1 and WS_2 = water surface elevation)

- Manning’s equation estimates the value of bed friction for the steady flow condition.
- The flow is the continuous function of the velocity and the water surface elevation H .

To simplify the calculation, the computing system of HEC-RAS assumes a horizontal water surface at each cross-section normal to the direction of flow such that the momentum exchange between the channel and the floodplain boundaries can be neglected (Dasallas et al., 2019). Kumar et al. (2017) and Dasallas et al. (2019) mentioned the following derivatives of 1D model (Fig. 13.3):

$$Y_2 + Z_2 + \frac{\alpha_2 V_2^2}{2g} = Y_1 + Z_1 + \frac{\alpha_1 V_1^2}{2g} + h_e \tag{13.1}$$

where Y_1 and Y_2 = flow depth of water (m), Z_1 and Z_2 = elevation of the main channel inverts (m), V_1 and V_2 = average velocity ($m\ s^{-1}$), α_1 and α_2 = velocity weighting coefficients, g = gravitational acceleration ($m\ s^{-2}$), and h_e = energy head loss (m).

De Saint Venant (1871) derived the following equations which is now used in HEC-RAS (Stelling & Verway, 2005; Fan et al., 2017):

$$\frac{\partial A_t}{\partial t} + \frac{\partial Q}{\partial x} = q_{lat} \tag{13.2}$$

$$\frac{1}{gA} \left\{ \frac{\partial Q}{\partial t} + \frac{\partial}{\partial x} \left(\frac{Q^2}{A} \right) \right\} + \frac{\partial \zeta}{\partial x} + \frac{Q|Q|}{K^2} = 0 \tag{13.3}$$

where A_t = cross-sectional area (m^2), t = time (s), Q = discharge ($m^3\ s^{-1}$), x = position along the channel axis (m), q_{lat} = lateral discharge per unit length of channel ($m^2\ s^{-1}$), A = flow-conveying cross-sectional area (m^2), ζ = water level

above a selected horizontal reference plane (m), and K = channel conveyance ($\text{m}^3 \text{s}^{-1}$). In its simplest form, Eq. (13.3) may be reduced to the familiar steady flow conveyance relationship

$$Q = K\sqrt{I} \quad (13.4)$$

with the conveyance K expressed as

$$K = CA\sqrt{R} \text{ or } K = \frac{1}{n}AR^{2/3} \quad (13.5)$$

where K is a function of Chezy resistance coefficient, hydraulic radius, cross-sectional area, and Manning's friction coefficient.

The set of Eqs. (13.2) and (13.4) forms the so-called *kinematic wave approximation* for flood propagation, which, after substitution of (13.4) into (13.2) and neglecting the lateral flow term, can be further simplified to the form

$$\frac{\partial Q}{\partial t} + c \frac{\partial Q}{\partial x} = 0 \quad (13.6)$$

with a flood wave celerity c (m s^{-1}) expressed as

$$c = \frac{1}{b_s} \frac{dQ}{dh} \quad (13.7)$$

4.2 Steps in Flood Inundation Model of HEC-RAS

The HEC-RAS 6.2 version software includes extreme number of hydrologic applications, mainly (1) steady and unsteady flow modelling, (2) analysis of both subcritical and supercritical flow regimes, (3) design of culvert and bridge, (4) bridge scour computation, (5) analysis of floodplain and channel area encroachment, (6) multiple profile computations, (7) sediment transport/movable bed modelling, (8) reservoir and spillway analysis, (9) X-Y-Z (pseudo 3D) graphics of the river system, (10) levee overtopping, etc. (Hicks & Peacock, 2005; Stelling & Verway, 2005; Merwade et al., 2008; Pramanik et al., 2010; Sarhadi et al., 2012; Sanyal et al., 2014b; Kumar et al., 2017; Patel et al., 2017; Teng et al., 2017; Pathan & Agnihotri, 2020; Singh et al., 2020). The goal of the flood inundation modelling is to evaluate the possible flood extent in a river reach using the basic functions of RAS Mapper in HEC-RAS to create a 1D model of a river system. To assist the decision makers or planners, the thematic maps of 1D hydrodynamic model is very significant to recognize the inundated areas of different flow regimes for mitigating floods, protection of cropland and settlements, and adapting flood-controlling measures in

reality. Flood inundation mapping needs high-resolution DEM (digital elevation model) or DTM (digital terrain model) database to maintain accuracy at field scale, and comparing the DEM of water with the DEM of ground the area of flooding is determined at all points where the water surface is above the ground surface (Merwade et al., 2008). The details of workflow and modeler application guide can be found in the technical document of US Army Corps of Engineers (2020). In this study the following steps are taken to execute 1D hydraulic model for flood inundation mapping (Merwade et al., 2008; Kumar et al., 2019):

1. Design steady flow (e.g., 2-year, 5-year, 15-year, and 25-year flood) is firstly estimated using a calibrated popular hydrologic model (log-Pearson Type III distribution), and an unsteady flow database is collected from the daily discharge data of a gauge station for a specific period.
2. The requirement of channel geometric data includes width, elevation, shape, length, location, geomorphic shape, boundary condition (Manning's coefficient), and slope. River floodplain data (digitizing main and tributary mid-channel part, left-right banks, channel confluence/bifurcation junction, and floodplain span) is firstly needed. The consecutive maximum numbers of downstream cross-sections (covering boundary of floodplain) are developed, creating river transects in DEM or DTM.
3. Step 1 (design steady or unsteady flow) and step 2 (channel geometry) are then processed in HEC-RAS to deduce water surface elevations (WSE) along the channel. Other hydraulic parameters are obtained by calibration.
4. The DEM is subtracted from the water surface to obtain a water-depth map. The area with positive values in the water-depth map gives the flood inundation map of different design flows.
5. Other main outputs of HEC-RAS modelling water velocity of design flows, flow area, cross-sectional view of WSE, and energy grade line slope.

4.3 Risk and Flood Frequency Analysis

For any hydrologic design, the estimation of risk and reliability is very essential task, and the hydrological risk can be used to fix the return period for a given design life, reflecting level of risk (Vogel & Castellarin, 2017). The probability of flood occurrence in any one year (event) is $p = 1/T$, and the probability of x occurrences in n years is $B(n, p)$. According to Vogel and Castellarin (2017), "the probability (at least one incidence in n events) is called risk which is defined as the probability that one or more events will exceed a given magnitude within a specified binomial distribution."

$$\text{Risk} = 1 - (1 - 1/T)^n \quad (13.8)$$

$$\text{Reliability} = (1 - p)^n = (1 - 1/T)^n \tag{13.9}$$

Nearly in all series of natural floods, the log-Pearson Type III (LPT3) distribution (similar to normal or Gaussian distribution) is applied as a commonly used frequency distribution for annual peak streamflow. The mean in LPT3 distribution is approximately equal to the logarithm of the 2-year peak discharge. The standard deviation is the slope of the line, and the skew is shown by the curvature of the line. The probability density function (PDF) of log-Pearson Type III distributed random variable is given by Rao and Hamed (2019):

$$f(x) = \frac{1}{\alpha x \Gamma(\beta)} \left[\frac{\log(x) - \gamma}{\alpha} \right]^{\beta - 1} e^{-\left\{ \frac{\log(x) - \gamma}{\alpha} \right\}} \tag{13.10}$$

where $f(x)$ = the probability density function, x = the variable in a Pearson III distribution (range $\gamma < x < \infty$), α and β = distribution location and scale parameters, and Γ = gamma function.

The distribution function of LPT3 distribution is given by the following equation (Rao & Hamed, 2000):

$$f(x) = \frac{1}{\alpha x \Gamma(\beta)} \int_0^x \frac{1}{x} \left[\frac{\log(x) - \gamma}{\alpha} \right]^{\beta - 1} e^{-\left\{ \frac{\log(x) - \gamma}{\alpha} \right\}} dx \tag{13.11}$$

If $y = \frac{\log(x) - \gamma}{\alpha}$ is substituted in equation, then we can get the equation

$$f(x) = \frac{1}{\Gamma(\beta)} \int_0^y \frac{1}{x} [y]^{\beta - 1} e^{-y} dy \tag{13.12}$$

In general form, the LPT3 distribution can be written as

$$Q_{LPT} = Q_{avg} + K_T S_l \tag{13.13}$$

where Q_{LPT} = logarithm of predicted discharge, at return period T , Q_{avg} = average of annual peak discharge logarithms, K_T = a function of return period (frequency factor) and skew coefficient, and S_l = the standard deviation of logarithms of annual peak discharge. K_T can be written as

$$K_T = \frac{2}{C_S} \left[\left\{ \frac{C_S}{6} \left(u - \frac{C_S}{6} \right) + 1 \right\}^3 - 1 \right], C_S > 0 \tag{13.14}$$

where u is the standard normal variate corresponding to a probability on non-exceedance of $P = 1 - 1/T$ and C_S is skew coefficient.

4.4 Other Hydrological Estimates

Daily runoff (Q_{Run}) of the ungauged basin can be calculated using NRCS-CN (Natural Resource Conservation Service Curve Number) method. Surface runoff for a particular rainstorm event is controlled by spatial pattern of land use–land cover (LULC) and hydrologic soil groups (HSG) which produce unique curve number (0–100) for a grid or a basin. An area-weighted average curve number is used for the entire catchment of Damodar to study the runoff effectively. The quantitative expressions of NRCS-CN method (Zade et al., 2005; Viji et al., 2015) can be written as

$$Q_{Run} = (\text{Rainfall} - 0.3 S_t)^2 / (\text{Rainfall} + 0.7 S_t) \tag{13.15}$$

$$S_t = 25,400 / CN - 254 \tag{13.16}$$

where S_t is potential maximum retention or recharge capacity after runoff begins (after 5 days antecedent rainfall condition).

In this study, the empirical formulae of flood peak potential (Q_{fpp}) are used to assess the probable maximum discharge of Damodar River, taking upper catchment basin area (19,920 km²) from the Rhondia gauge station. Alongside, other hydrological estimates and indices related to flood hydrology are given in Table 13.3. It is needed to mention that two nonparametric methods (Mann-Kendall and Sen’s slope estimator) were used to detect the significant trends of annual rainfall and annual peak discharge. The Mann-Kendall statistical test (M-K Test) and Sen’s slope (Kamal & Pachauri, 2019; Saikia & Konwar, 2020) are used here to quantify the significance of trends in hydrometeorological time series (viz., annual rainfall and annual peak discharge). Positive values of Kendall T (tau) indicate increasing trends,

Table 13.3 Important quantitative indices of flood hydrology

Sl. no.	Empirical formula and index	References
1	Dickens formula: $Q_{flood} = C_D A^{3/4}$, where Q_{flood} = estimated maximum flood peak (m ³ s ⁻¹), C_D = Dickens constant (range: 6–30), and A = catchment area (km ²)	Raghunath (2006)
2	Inglis formula: $Q_{flood} = 124 A / (A + 10.4)^{0.5}$	Raghunath (2006)
3	World envelope curve: $Q_{flood} = 3010 A / (277 + A)^{0.78}$	Subramanya (2013)
4	Indian envelope curve: $Q_{flood} = 4897 A^{0.19}$	Rakhecha and Singh (2017)
5	$C_v = \sigma / X_{mean}$, where C_v = coefficient of variation, X_{mean} = mean annual peak discharge, and σ = standard deviation	Raghunath (2006)
6	$C_s = \Sigma(X_i - X_{mean})^3 / (n - 1) \sigma^3$; C_s = coefficient of skew, X_i = each observation of annual peak discharge, and n = number of observations	Raghunath (2006)
7	$C_f = X_{mean} A^{0.8} / 2.14$; C_f = coefficient of flood	Raghunath (2006)

while negative T values show decreasing trends. In this study, significance levels $\alpha = 0.01$ and $\alpha = 0.05$ were used. At the 5% significance level, the null hypothesis of no trend is rejected if $|T| > 1.96$ and rejected if $|T| > 2.576$ at the 1% significance level. Alongside estimating statistically significant range of peak discharge, the confidence interval (CI) at 99% significance is applied here:

$$CI = X_{\text{mean}} - 3\sigma/\sqrt{n} \text{ to } X_{\text{mean}} + 3\sigma/\sqrt{n} \quad (13.17)$$

5 Results

5.1 Analysis of Flood Climate

The terms “flood climate” (Hayden, 1988) and “flood hydroclimatology” (Hirschboeck, 1988) include detail focus on the regional climate and atmospheric activity which promotes recurrent flood condition in connection with changing climate of the regions. Tropical climate, including monsoon climate of India, has high potentiality of torrential rainfall within a short period, which can instigate massive flood flows of Indian rivers. The flood climate of India can be designated as $Tszo$ type (Hayden, 1988) in which barotropy (T), seasonal basis (s), intertropical convergence zone, (z) and organized convective activity at synoptic scale (o) are key determinants (Ghosh, 2013). The rainfall maps (Fig. 13.4) of DRB and associated basins (1990–2020) express that trend of mean annual rainfall increases from west to east direction and the maximum annual rainfall of the eastern basin varies from 1662 to 1977 mm (minimum annual rainfall of western basin: 790–1309 mm). In monsoon months (June–October), the rivers experience floods annually after a spell of heavy rainfall (150–300 mm within 3–4 days) because this amount of rainfall yields a gigantic volume of runoff in respect of catchment’s physical characteristics. Today’s climate is occurring in an atmosphere that’s been made warmer, wetter/humid and more energetic. Due to global warming input of more heat energy to atmosphere promotes more moisture in the air. It is learned that for every degree of warming, the atmosphere can hold around 7% more moisture (Climate Signals, 2022), and more rainfall comes in short with intense downpours, which has increased the risk of flash floods in India. The 2010 report by the Ministry of Environment and Forests, Government of India stated that India’s average temperature has risen by around 0.7 °C during 1901–2018. Due to climate change the summer monsoon precipitation (June–September) over India has also weakened by around 6% from 1951 to 2015 with notable decrease of annual rainfall (but increase of extreme rainfall event for a short period) over the Indo-Gangetic Plains (Sahoo & Bhaskaran, 2016). Interestingly, in the world, the number of rainy days is declining, while intense rainfall events of 10–15 cm per day are escalating (Chattopadhyay et al., 2020). This means that more amount of water is pouring downs in lesser time, and it creates maximum

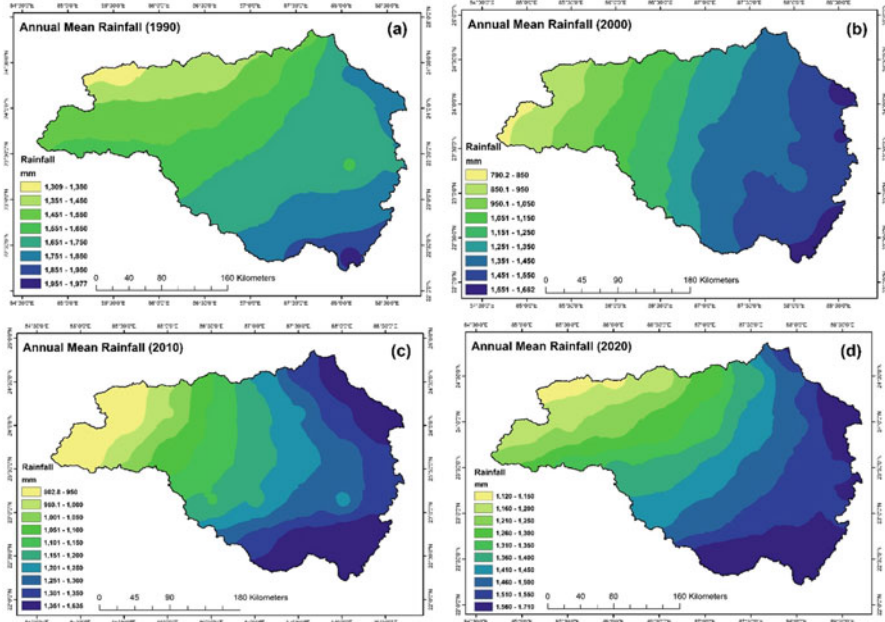


Fig. 13.4 Areal distribution of mean annual rainfall (decreasing trend from west to east) in 1990 (a), 2000 (b), 2010 (c), and 2020 (d) over the Damodar River Basin and other associated basins

level of flood risk in the tropical region. In a nutshell, climate change has extreme impacts in India: (a) rise in average temperature, (b) trend of no rain for long period, (c) sudden burst of excessive heavy rainfall, and (d) occurrence of extreme weather hazard, like flash floods of Himalayas and monsoon floods of Ganga and Brahmaputra Basins.

Alongside, the tropical depressions and cyclones are another factor of heaviest rainfall and flood in India. The lower Ganga basin, including DRB, experiences west-north-westwards tracks of depressions and cyclones from the head of the Bay of Bengal to the Chhotangapur Plateau, causing heavy rainstorms and downpours throughout the region of West Bengal and Jharkhand. Tropical cyclone activity (development of depression and cyclonic storm) during late monsoon period shows an upward trend and also exhibits El Nino Southern Oscillation (ENSO) of 2–5 years’ time scale over the Bay of Bengal (Sahoo & Bhaskaran, 2016). Track of cyclone and depression is very much linked to occasional extreme floods of DRB, because in many cases (viz., floods of October 1978, June 1981, September 2000, September 2009, August 2016, and May 2021), the path of cyclonic activity moved from downstream to upstream direction (southeast to northwest) along the entire basin. In between 1986 and 1995, the track was mostly northward and then westward from the Bay of Bengal, and it covered the DRB and its associated basins. During 2006–2015, most cyclones moved northward. A key fact of DRB is that during cyclonic rainfall (moving southeast to northwest), the lower basin (West Bengal) is

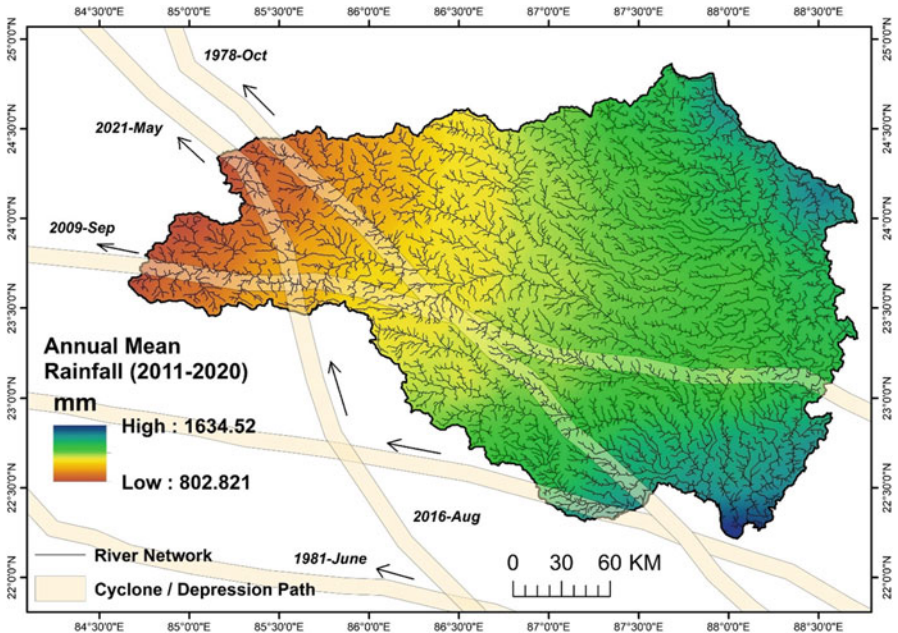


Fig. 13.5 Tracks of tropical cyclones and depressions over the rainfall region of Damodar River Basin

already saturated with high moisture, and alongside when the cyclone reaches at the upper basin (Jharkhand), the region also experiences heavy rainfall (110–230 mm in 3–4 days) due to high topographic lift (>600 m from mean sea level) causing the excessive concentrations of runoff (later flood flow) in the fluvial system of Damodar and Barakar (Fig. 13.5).

W.W. Hunter (1876), in his Statistical Account of Bengal, described Damodar floods as *harka ban* (flash flood) having floodplain inundation depth of 1.5 m in the lower basin. Floods in the DRB have been presented as an aberrant and unpredicted behavior of the river, making “river training,” “river control,” “taming,” and “harvesting” of it very problematic and of then critical for a decade (Majumder et al., 2010b). In documentation, the great floods of Damodar were almost recurrent phenomena at past – 1770, 1855, 1866, 1873–1874, 1875–1876, 1884–1885, 1891–1892, 1897, 1900, 1907, 1913, 1927, 1930, 1935, 1943, 1959, 1978, 2000, 2011, 2016, and 2021 (Majumder et al., 2010b). Bardhaman town and its adjoining region were completely flooded in 1770, 1855, 1913, and 1943 having discharge of more than $16,000 \text{ m}^3 \text{ s}^{-1}$. To save the land from flood, the embankment was stated to build between 1866 and 1873 under the leadership of Maharaja Kirti Chand of Bardhaman. After independence of India, the flood hydrology of the Damodar catchment was getting more importance in view of India’s first multipurpose river valley project being undertaken in the basin adapting the model of Tennessee Valley Authority (TVA). The extensive studies of Glass (1924), Kirk (1950), Pramanik and

Table 13.4 Historical record of seven rainstorms and resulting flood flows in the Damodar River at Raniganj

Sl. no.	Date of occurrence of rainstorm	No. of days rainfall	Date of occurrence of floods	Mean rainfall (mm)	Mean discharge (m^3s^{-1})	Peak discharge (m^3s^{-1})
1	28th Aug–31st Aug, 1909	4	31st Oct–1st Sept	116.84	5017	10,109
2	5th Aug–10th Aug, 1913	5	6th Aug–14th Aug	299.72	5663	18,406
3	21th Sep–7th Oct, 1916	6	22nd Sep–28th Sep	162.56	3879	11,128
4	1st Oct–25th Sep, 1916	5	2nd Oct–9th Oct	119.38	2832	6711
5	29th Jul–2nd Aug, 1917	5	30th Jul–4th Aug	243.84	4814	8070
6	30th Sep–7th Oct, 1917	8	1st Oct–12th Oct	248.92	4106	10,902
7	29th Oct–31st Oct, 1917	3	30th Nov–1st Nov	68.58	3398	6050

Rao (1952), Chatterjee (1967), Bhalla (1969), Sinha and Rao (1985), and Bhattacharya (2011) made few conclusions regarding the unique characteristics of flood climate in the DRB:

1. Key driver of each miserable flood is the torrential rainfall over the upper catchment. Total mean rainfall on the whole catchment producing floods generally varies from 76.2 mm in 3 days to a maximum of about 304.8 mm in 6 days. It is assumed that a maximum extreme rainfall of 508 mm in the first half of the monsoon season and 127 mm in the latter half with runoff coefficient of 90%.
2. An intensive rainstorm giving more than 330.2 mm of mean rainfall over the upper catchment may occur once in about 65 years and one giving more than 381 mm once in about 120 years. A storm giving 457.2 mm rainfall in 6 days of which 330.2 mm may fall in 3 days and 177.8 mm in a day may be assumed as the maximum that is likely to occur over the upper catchment.
3. A rainstorm magnitude equal to or greater than 304.8 mm occurs once in 100 years and greater than 355.6 mm in 250 years. Further, a storm rainfall giving 411.48 mm is likely to be equaled or exceeded only once in 1000 years. Between 1891 and 1980, 1 day maximum rainfall recorded as 124.71 mm and 7 days maximum rainfall recorded as 312.93 mm in the DRB.

Pre-dam historical data and analysis (Glass, 1924; Pramanik & Rao, 1952) is very much needed to understand and predict the flood condition. The following lessons are learnt from the past records (Table 13.4):

1. The maximum recorded 3-day rainfall was about 254 mm at pre-dam period. That rate of rainfall for the Damodar catchment of 18,648 km^2 work out to an average rate of peak discharge 18,264 m^3s^{-1} at Raniganj.

2. High discharge at Rhondia (exceeding $5663 \text{ m}^3\text{s}^{-1}$) on any date is very highly correlated with the rainfall recorded on the date and the preceding 2 days. It is formulated a regression trendline between rainfall (R , inches) of July to October with the corresponding seasonal flow (D , cusec) expressed during pre-dam period: $D = 0.65 R - 8.68$.
3. Discharge of the Damodar River at Rhondia on any day is very much correlated with the following: (a) rainfall of preceding day (0.73), (b) rainfall of preceding 2 days (0.80), and (c) rainfall of preceding day and discharge of preceding day (0.82). Two linear relationships are established: (a) $D = 4.35 (R_{-1} + R_{-2}) + 0.9703$ and (b) $D = 71.70 R_{-1} + 14.6787$.
4. From 1909 to 1917 it was observed that 3–8 days continuous mean rainfall of 68.58–299.72 mm produced a peak flood discharge range of 6060–18,406 m^3s^{-1} at Raniganj (table).

It was estimated that Damodar catchment received monsoon rainfall (June–October) of 855.57–1043.55 mm and Barakar catchment received monsoon rainfall of 840.54–1079.81 mm annually (Ghosh & Mistri, 2015). In between 1950 and 2000, the Jharkhand division of DRB received mean annual rainfall of 1091 mm, and the part of West Bengal receives 1167 mm. CHRS data of 2001–2020 period shows that mean normal annual rainfall of upper catchment ranges in between 1219 mm (western part) and 1923 mm (eastern part), reflecting an increasing trend of annual rainfall than previous (Fig. 13.6a). Rainfall trends in the DRB over the period of 46 years (1970–2015) reflect summer monsoon rainfall accounting for around 80% of total rainfall and increasing rainfall trend in post-monsoon season (Chattopadhyay et al., 2020). Total DRB receives quite same annual rainfall in between 1970 and 2015, and it is increasing from past record, reflecting high chance of flood risk: (1) Damodar catchment – 1298 mm (14.4–18.3% positive change); (2) Barakar catchment – 1267 mm (11.7–19.1% positive change); and (3) lower Damodar catchment – 1339 mm (12.1–16.6% positive change). Mann-Kendall test and Sen's slope reveal a significant increasing trend in annual rainfall: (1) 1.64–3.78 mm year^{-1} in the Barakar catchment, (2) 0.85–2.32 mm year^{-1} in the Damodar catchment, and (3) 0.46–4.80 mm year^{-1} in the lower Damodar catchment (Table 13.5).

Now, the analysis is concentrated on the post-dam records of flood events which reflect the spatial concentration of 3–4 days flood producing rainfall and the resultant peak discharge at Rhondia. The mean annual rainfall (2001–2020) of the upper catchment varies from 1219 to 1923 mm (Fig. 13.6a) which is exceptionally extortionate, signifying high moisture laden basin area. Four distinct maps of flood events are taken into consideration to depict the moisture condition over the upper catchment during short period of heavy rainfall:

- Seven days (17th–23rd September, 2000) continuous rainfall of 34–290 mm was received in the Damodar and Barakar catchment due to tropical depression (Fig. 13.6b). The most intense rainfall of 251–290 mm was recorded around the Panchet and Maithon reservoirs. That period of cumulative rainfall generated maximum peak discharge of $6387 \text{ m}^3 \text{ s}^{-1}$ at Rhondia on 23rd September, 2000.

Fig. 13.6 Spatial distribution of rainfall over the upper catchment of Damodar: (a) mean normal rainfall distribution of period 2001–2020 in the upper catchment of Damodar, showing west–east increasing trend, (b) an event of maximum 290 mm rainfall (September, 2000) generated streamflow of $6387 \text{ m}^3 \text{ s}^{-1}$, (c) an event of maximum 268 mm rainfall (September, 2006) generated streamflow of $7035 \text{ m}^3 \text{ s}^{-1}$, (d) an event of maximum 203 mm rainfall (September, 2007) generated streamflow of $8883 \text{ m}^3 \text{ s}^{-1}$, and (e) an event of maximum 235 mm rainfall (August, 2011) generated streamflow of $5211 \text{ m}^3 \text{ s}^{-1}$

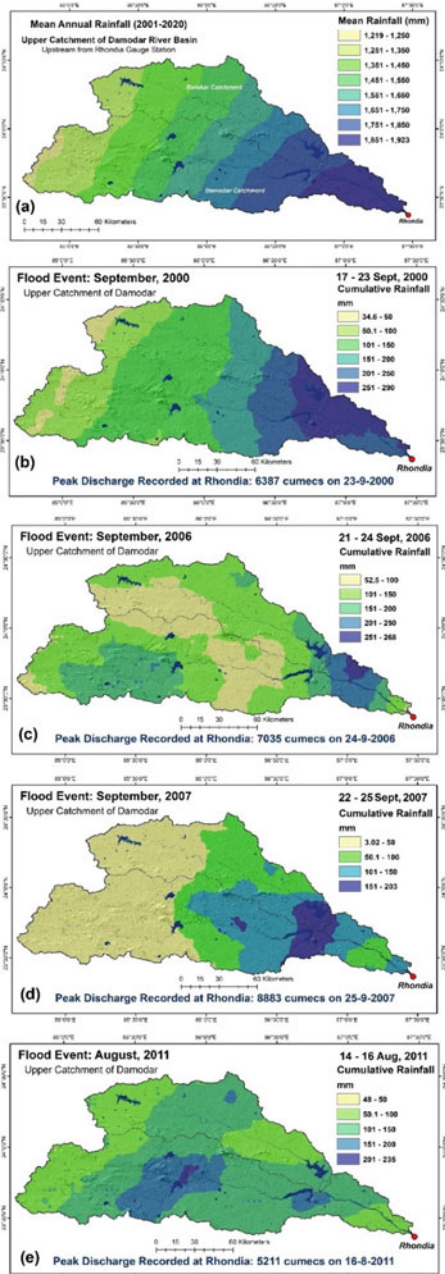


Table 13.5 Summary of rainfall record (1970–2015), M-K Test, and Sen's slope in the DRB

Catchment	Station	Mean annual rainfall (mm)	SD	CV (%)	M-K Test Z value	Trend	Sen's slope (mm year ⁻¹)
Barakar	Maithon	1272	204	16	1.36	+	1.64
	Tilaiya	1273	198	16	0.98	+	1.56
	Barkisuriya	1280	203	16	1.43	+	3.78
	Barhi	1243	190	15	1.40	+	2.65
Damodar	Panchet	1307	189	15	1.05	+	2.32
	Sindri	1305	191	15	0.68	+	0.85
	Bokaro	1283	191	15	0.96	+	1.87
	Hazaribagh	1302	190	15	0.77	+	1.35
Lower Damodar	Asansol	1336	236	18	0.33	+	0.46
	Durgapur	1338	237	18	0.68	+	1.42
	Bardhaman	1340	235	17	0.71	+	3.75
	Uluberia	1342	235	17	0.81	+	4.8

Data source: Chattopadhyay et al. (2020)

SD standard deviation, CV coefficient of variation

- Four days (21st–24th September, 2006) rainfall varied from 52.5 to 268 mm, and the Damodar catchment received alone cumulative rainfall of 201–268 mm (Fig. 13.6c). After DVC flow regulation on 24th September, 2006, the recorded peak discharge was 7035 m³s⁻¹.
- Four days period (22nd–25th September, 2007) of 50–203 mm rainfall (Fig. 13.6d) generated maximum peak discharge of 8883 m³s⁻¹ at Rhondia. The region around Panchet and Maithon reservoirs contributed more than 151 mm rainfall within 4 days.
- From 14th to 16th August, 2011, the upper catchment received rainfall of 48–235 mm (Fig. 13.6e), and more than 101 mm rainfall was recorded over the Damodar catchment within 3 days. During that rainfall event, the Durgapur Barrage was compelled to release maximum peak discharge of 5211 m³s⁻¹ on 16th August, 2011.

Finally, an exponential relationship between peak discharge (Q_{peak}) and 3–4 days cumulative rainfall of upper catchment (R_{cum}) is established on the basis of post-dam flood records:

$$Q_{\text{peak}} = 2213.1e^{0.0038 R_{\text{cum}}} (R^2 = 0.6838) \quad (13.18)$$

From this empirical relationship a forecast of flood-generating rainfall is developed for 2-year, 10-year, 50-year, and 100-year floods (design flood developed using log-Pearson Type III distribution) in the DRB:

1. 2-year flood (3254 m³s⁻¹): 205 mm rainfall
2. 10-year flood (6676 m³s⁻¹): 304 mm rainfall
3. 50-year flood (9417 m³s⁻¹): 360 mm rainfall
4. 100-year flood (11,969 m³s⁻¹): 412 mm rainfall.

5.2 Impact of Dam on Hydrological Variability

Few significant studies (Glass, 1924; Bhattacharya, 2011, Ghosh & Mistri, 2015; Ghosh & Guchhait, 2016; Karim & De, 2019; Singh et al., 2019) revealed the dam-induced changes in annual hydrograph, streamflow, and maximum flood discharge of the Damodar River. Here, a number of important hydrologic observations are presented to know the flood hydrological variability of a dam-controlled river. Annual hydrograph (Fig. 13.7a) of pre-dam (1934–1957) and post-dam (1958–2015) shows a marked shifting of peak monsoon flow from August to

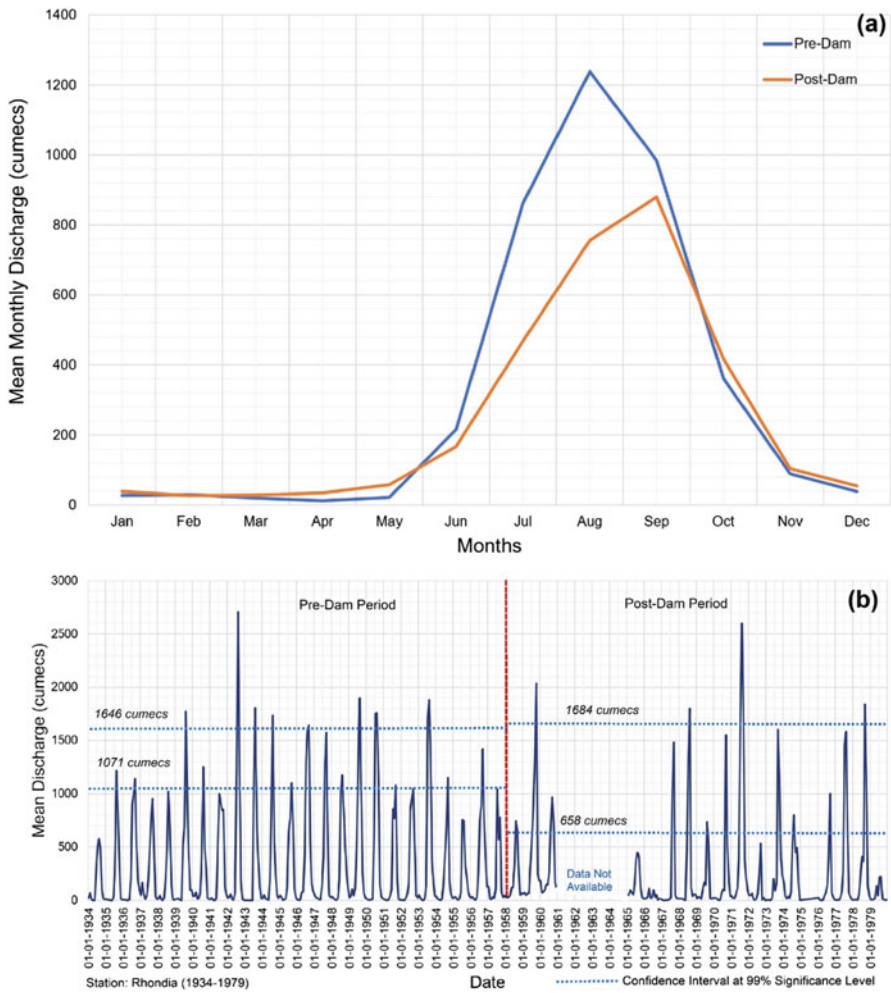


Fig. 13.7 (a) Annual hydrograph of pre-dam and post-dam period based on mean monthly discharge and (b) marked variability of mean discharge during pre-dam and post-dam period, delimiting confidence intervals of discharge

September due to flow regulation of DVC dams. To maintain flood storage of first half monsoon, the DVC dams are now compelled to release excess water during 2nd half of monsoon. It also reflects the changing period of flood occurrence: (1) pre-dam maximum likelihood of flood event was August, and (2) post-dam maximum likelihood of flood event is September. Due to dam-controlled flow regulation, the average monthly peak flow is now reduced up to 28.94% from the previous natural condition (decreased from 1238 to 879 m^3s^{-1}). Mean monthly discharge of Damodar River was regulated by DVC dams since 1958. Pre-dam pre-monsoon base flow was near about 12.16 m^3s^{-1} , but dam regulation has maintained a base flow of 34.41 m^3s^{-1} (Fig. 13.7b). Under natural condition, the mean monsoon peak discharge was greater than 1500 m^3s^{-1} in a number of cases, but that value has reduced significantly in post-dam period.

In natural condition, the Damodar River had high potentiality to cause violent flood flow. Between 1934 and 1948, the highest recorded average peak discharge was 14,767 m^3s^{-1} on 10 October, 1941 (Fig. 13.8a). Another peak discharge of 18,123 m^3s^{-1} was recorded on 12th August, 1935. Pramanik and Rao (1952) estimated that in the pre-dam period, a maximum discharge of 28,317 m^3s^{-1} could be likely exceeded once in about 850 years. From 1823 to 1942, 12 times the peak discharge of flood events reached beyond 10,000 m^3s^{-1} and during 5 times the river experienced discharge beyond 17,000 m^3s^{-1} . A significant variation of annual peak discharge time series is observed. Since 1823, 13 times the annual peak discharge or extreme flood flow crossed 10,000 m^3s^{-1} in the Damodar River, reflecting violent nature of flood. In pre-dam period (1933–1957), calculated *CI* (at 99% significance level) varied from 6055 to 10,459 m^3s^{-1} (range – 4404 m^3s^{-1}) which is considered an exceptional high flow as compared to present condition (Fig. 13.8b). Since 1958, the DVC dams have effectively reduced *CI* which now ranges between 2790 and 4511 m^3s^{-1} (range – 1721 m^3s^{-1}), reducing the maximum likelihood flood flow up to 53.92–56.87% in the river. Importantly the post-dam time series shows a positive growth trend (1958–1978 and 1979–2015) which matches with increasing trend of annual rainfall in the DRB since 1970 (as discussed in pervious section). M-K test is performed on two separate time series ($N = 21$ and $N = 37$), separated on the basis of maximum 1978 flood flow (10,919 m^3s^{-1}); Kendall tau (0.1238 and 0.2012) shows significant (rejecting null hypothesis and accepting alternative hypothesis, i.e., slope is not zero at 0.05 significance level) but weak time series trend (Table 13.6). The positive *Z* value, 0.75492 and 1.7395. expresses an increasing trend of annual peak discharge with time. Sen's slope of two time periods is expressed as: (i) 44.487 m^3s^{-1} per year (1958–1978) and (ii) 46.639 m^3s^{-1} per year (1979–2015).

Apart from the annual peak discharge analysis, NRCS-CN output exhibits the spatial variability of curve number (*CN*) and surface runoff depth in the selected flood events of 2000 and 2006 to portray the regions of maximum water concentration (or excess water coming from which areas in the upstream watershed of Panchet and Maithon dams). The runoff curve number (i.e., *CN* is an empirical parameter used for predicting direct runoff during a rainfall event) is primary guided by the HSG and LULC which are mapped in the upper catchment of Damodar. GIS analysis suggests that a maximum area of 17,011 km^2 (85.39% of total upper

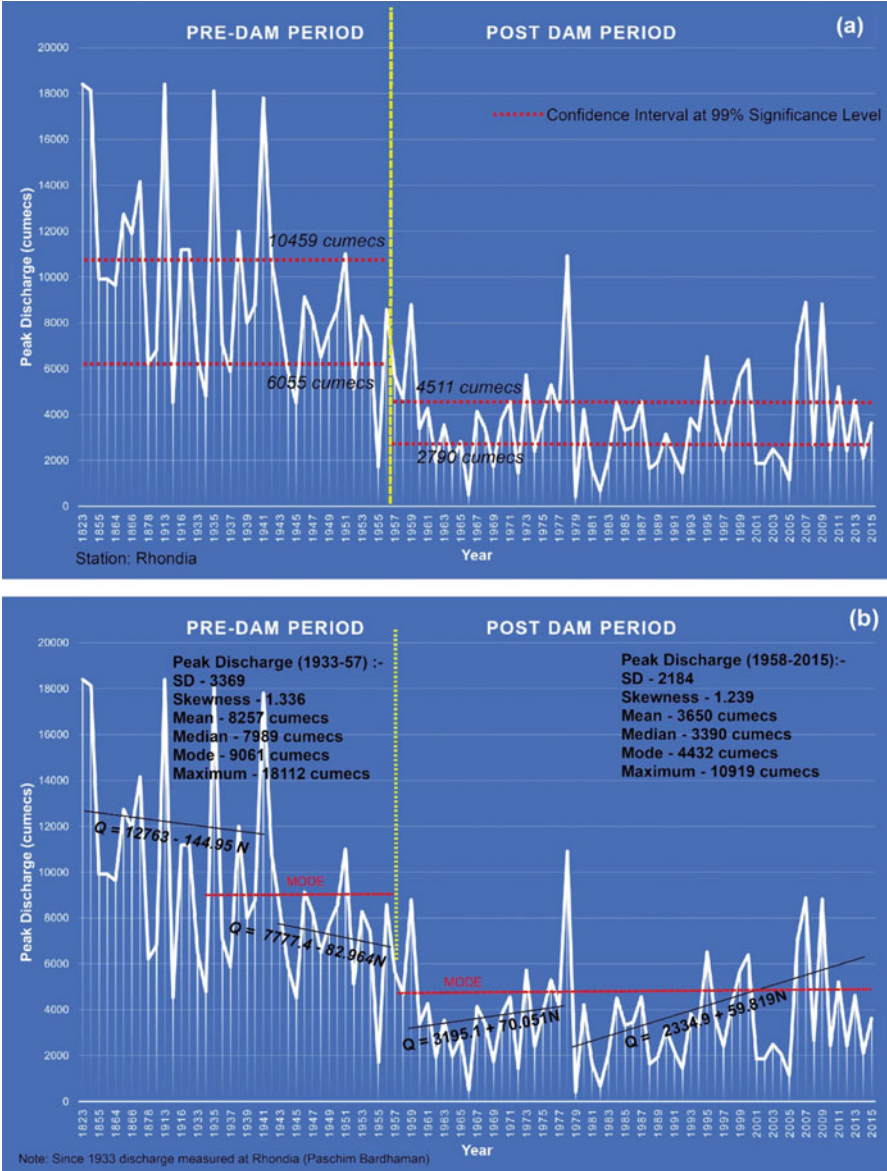


Fig. 13.8 (a) Erraticism between natural annual peak flow regime and dam-induced changes in annual peak flow, delimiting marked variation of confidence intervals, and (b) observed trends of annual peak flow during pre- (decreasing) and post-dam period (increasing), including variations of hydrological statistics

Table 13.6 M-K test and Sen's slope analysis for post-dam annual peak discharge time series

Parameters	Time period (1958–1978)	Time period (1979–2015)	Remarks
N	21	37	Rejecting null hypothesis and accepting alternative hypothesis, i.e., slope is not zero at 0.05 significance level, an increasing trend (+) in time series of post-dam period
Z	0.7549	1.7395	
p -value	0.4503	0.0819	
S	26	134	
Var S	1096.66	5846	
Tau	0.1238	0.2012	
Sen's slope	44.487	46.639	
Sen's slope at 95% confidence interval	– 104.545–226.000	– 6.166–110.863	

catchment area) is categorized as HSG C (viz., loam, sandy clay loam, silt loam, clay loam, and silty clay loam soil textures), and other categories are HSG D (463 km²), HSG C/D (319 km²), and D/D (56 km²). In the catchment, an area of 4948 km² (24.84% of total upper catchment area) is designated as natural vegetation and forest cover, and the area of cropland and seasonal fallow land covers 9702 km² (48.71% of total area). Alongside, other LULC classes are designated as waterbodies/rivers (525 km²), grassland (40 km²), scrub/shrub/bushes (2178 km²), flooded vegetation (34 km²), bare land (42 km²), and built-up/settlement (2493 km²), respectively. Using Python programming in ArcGIS 10.4, the weighted CN (0–100) is derived for the upper catchment from the raster database of HSG and LULC. The mean weighted CN of the catchment is 78.57 which signifies quite high runoff potentiality of the hard rock terrain. The CN map reflects the maximum coverage of range 51–75, followed by range 76–100 (Fig. 13.9a). The runoff maps of rainfall events of September, 2000 and September, 2006 exhibit the following findings:

- *First case:* The total rainfall, during 13–23 September, 2000, varied widely from 34 to 290 mm (Fig. 13.9b), and it had maximum record (>201 mm) around the adjoining parts of Panchet and Maithon dams. For that amount of 7 days cumulative rainfall that parts of catchment yielded potentially 151–200 mm runoff, having extreme concentration of 201–282 mm runoff at selected pockets. That amount of runoff on a vast region accumulated in the DVC reservoirs, and finally, the dams were compelled to release excess water at the rate of maximum 6387 m³s⁻¹ on 23 September, 2000 in the Damodar River, inundating the lower valleys of Purba Bardhaman, Hooghly, and Howrah districts.
- *Second case:* The 4 days total rainfall, from 21 to 24 September, 2006, ranged between 52.5 and 268 mm (Fig. 13.9c), and the torrential rainfall of >151 mm was observed in the hilly tract of Damodar catchment and downstream of Panchet and Maithon dams. That amount of heavy rainfall yielded a runoff range of 10–207 mm, having extreme concentration (>101 mm) around those parts. As a result, on 24 September, 2006, the recorded maximum discharge of Damodar was 7035 m³s⁻¹, causing havoc flood in the low-lying floodplains of Hooghly and Howrah.

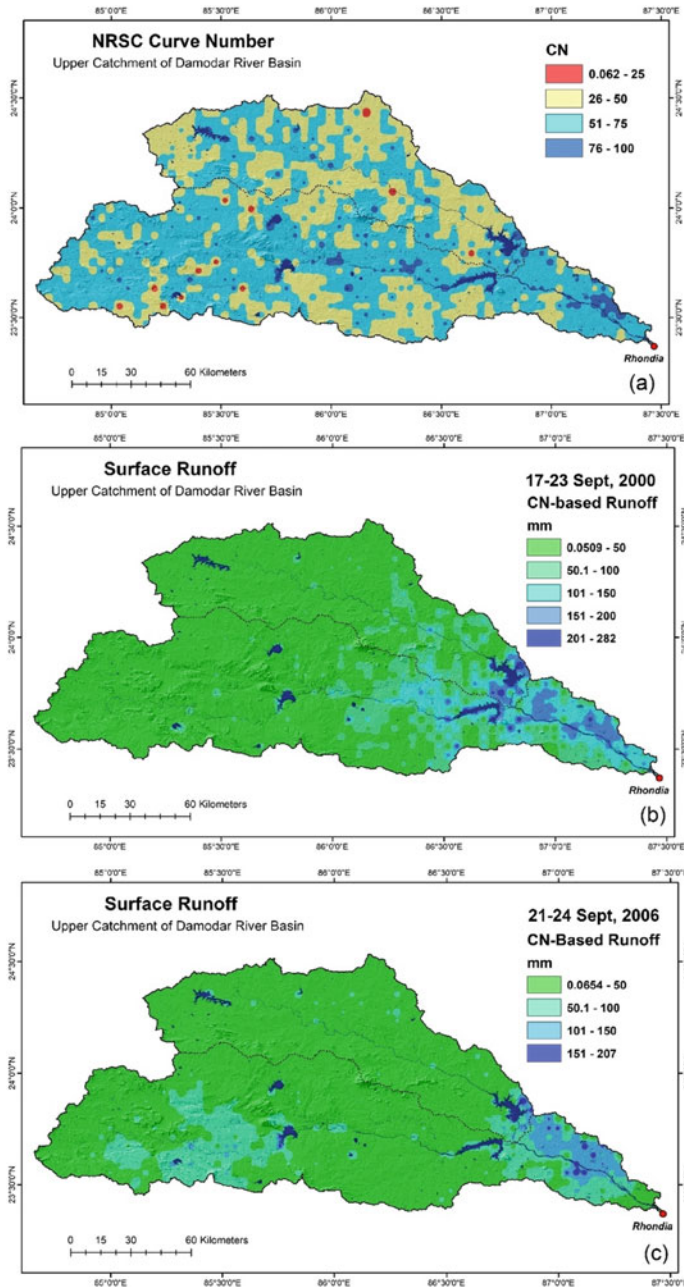


Fig. 13.9 (a) An important and useful map of weighted NRCS curve numbers developed for the upper catchment of Damodar (including basin area of Barakar River), (b) spatial extent of CN-derived potential runoff (50–282 mm) during the flood event of 17–23 September 2000, and (c) spatial extent of potential runoff (50–207 mm) during the flood event of 21th–24 September 2006

5.3 Flood Frequency and Hydrological Risk

The empirical formulae of predicting maximum flood peaks (Table 13.1) have yielded variable results for the Damodar River (considering 19,920 km² of catchment area from Rhondia gauge station): (i) Dickens result – 23,474 m³s⁻¹; (ii) Inglis result – 17,455 m³s⁻¹; (iii) world envelope curve result – 26,286 m³s⁻¹; and (iv) envelope curve of Rakhecha and Singh result – 32,121 m³s⁻¹. The maximum recorded flood peak in pre-dam period was 18,406 m³s⁻¹ (1913), and in post-dam period it was 10,919 m³s⁻¹ (1978). So, the observed value is very much close to the result of Inglis empirical formula. In this study, two different time series (annual peak discharge of pre-dam and post-dam) of two stations (Rhondia and Harinkhola) are taken into consideration for flood frequency analysis (FFA). From the pre-dam (1933–1957) and post-dam (1958–2015) database of Rhondia station, it is estimated that in pre-dam period, i.e., natural condition, there are a greater number of floods above the mean peak discharge (7413 m³s⁻¹) than the post-dam period mean (3650 m³s⁻¹). The curve which fits the annual peak flood discharge data on a log-log paper will not be a symmetrical curve, but a skew curve which unsymmetrical, i.e., points do not lie on the straight line but the line bends off. The general slope of this curve is given by the coefficient of variation (C_v), and the departure from the straight line is given by the coefficient of skew (C_s). In pre-dam period the smaller value of C_v (0.312) indicates occurrence of floods in same magnitude, but large C_v (0.592) of post-dam period reflects a range in the magnitude of floods due to dam control. The coefficient of flood (C_f) indicates the general magnitude of the floods above one unit in the particular river; it fixes the height of the nonlinear curve above the base. In pre-dam period C_f was extremely huge, i.e., 5.767, but after dam construction it reduces to 2.855, decreasing (49.50%) the flood curve height significantly.

Distribution of annual peak discharge fits well log-Pearson Type III (LPT3) distribution, as significant in Goodness-of-Fit test, in the case of DRB. The output shows very less deviation of LPT3 predicted flow (Q_{pred}) in respect of observed flow (Q_{obs}), fitting a linear relationship of $Q_{\text{pred}} = 88.515 + 0.9758 Q_{\text{obs}}$ ($R^2 = 0.9757$). The hydrological risk, associated with FFA, is assessed here in terms of reoccurrence interval and exceedance of probability measures. The results of FFA exhibit a notable predictability of flood design in respect of pre-dam (1933–1957) and post-dam (1958–2015) probability distribution. The key statistical findings are mentioned as follows:

1. There is a reduction (up to 55.79%) of mean annual peak discharge (Q_{peak}) or flood flow from pre-dam to post-dam period due to the regulated control of DVC dams during the monsoon months. The weighted skewness (C_w) of pre-dam period is -0.51074 which was transformed to very high, i.e., 2.234, during post-dam period, signifying high range between flood magnitude. Another LPT3 derived parameter is coefficient of skewness (C_s) which is exceptionally very high (3.6962) during pre-dam period, but after dam construction due to flow regulation and flood reserve of reservoirs C_s reduces to -0.757 . Kurtosis of

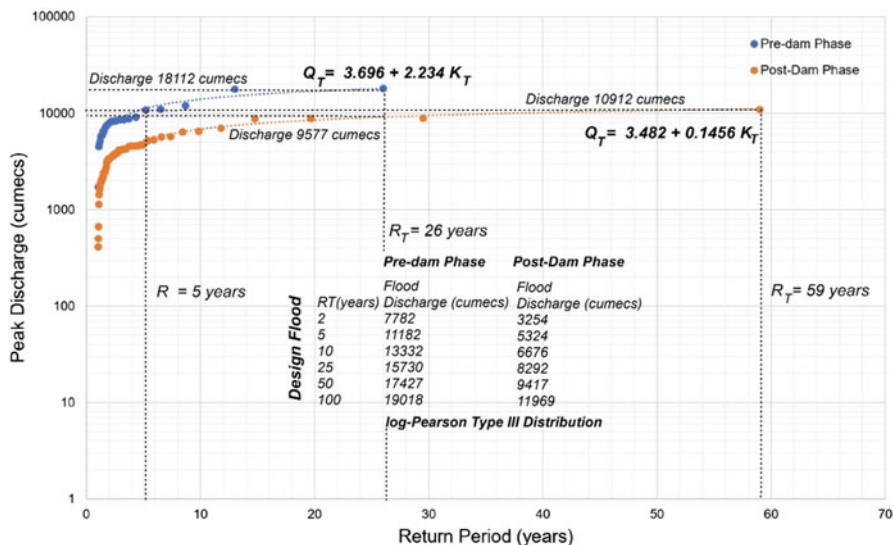


Fig. 13.10 Variability of LPT3 flood frequency distribution in pre- and post-dam period, showing estimated changes in design floods and return periods

pre-dam period is 1.776 which changed to 2.625 in post-dam period. In both cases, kurtosis reflects a fat-tailed distribution (leptokurtic), having very high skewness and high degree of peakedness of the flood frequency distribution with high probability of extreme outlier values (i.e., maximum likelihood of flood events).

- LPT3 shows that the annual peak discharge of less than $5658 \text{ m}^3\text{s}^{-1}$ (during pre-dam period) occurs with an exceedance probability of greater than 80%, but in post-dam period the 80% exceedance probability of flood occurrence is reduced to only $1897 \text{ m}^3\text{s}^{-1}$ in the Damodar River. It is noteworthy to mention that an extreme peak flow of $10,919 \text{ m}^3\text{s}^{-1}$ (observed in 1978) can be occurred having only 1.69% chance (in any one year) at present condition and that flow had 19.34% probability of occurrence during pre-dam period (Fig. 13.10).
- Recurrence interval or return period (R_T) provides the estimated interval between events of a similar size or intensity of flood. In pre-dam period, a flood flow of $18,112 \text{ m}^3\text{s}^{-1}$ (observed in 1935) has 26 years R_T , and it has 3.846% chance of being exceeded in any one year. The pre-dam flow of $4514 \text{ m}^3\text{s}^{-1}$ has only R_T of 1.08 years (almost regular event), having 92.30% chance of being exceeded in any one year. A 100-year flood, a flood event that has 1% probability or 1 in 100 chances of being equalled or exceeded in any given year, is estimated about $19,018 \text{ m}^3\text{s}^{-1}$. Alongside, FFA estimates the 2-year flood was $7782 \text{ m}^3\text{s}^{-1}$ having 50% chance of occurrence in one of given years. It shows the propensity of past furious floods with a maximum likelihood of occurrence in the DRB. For that

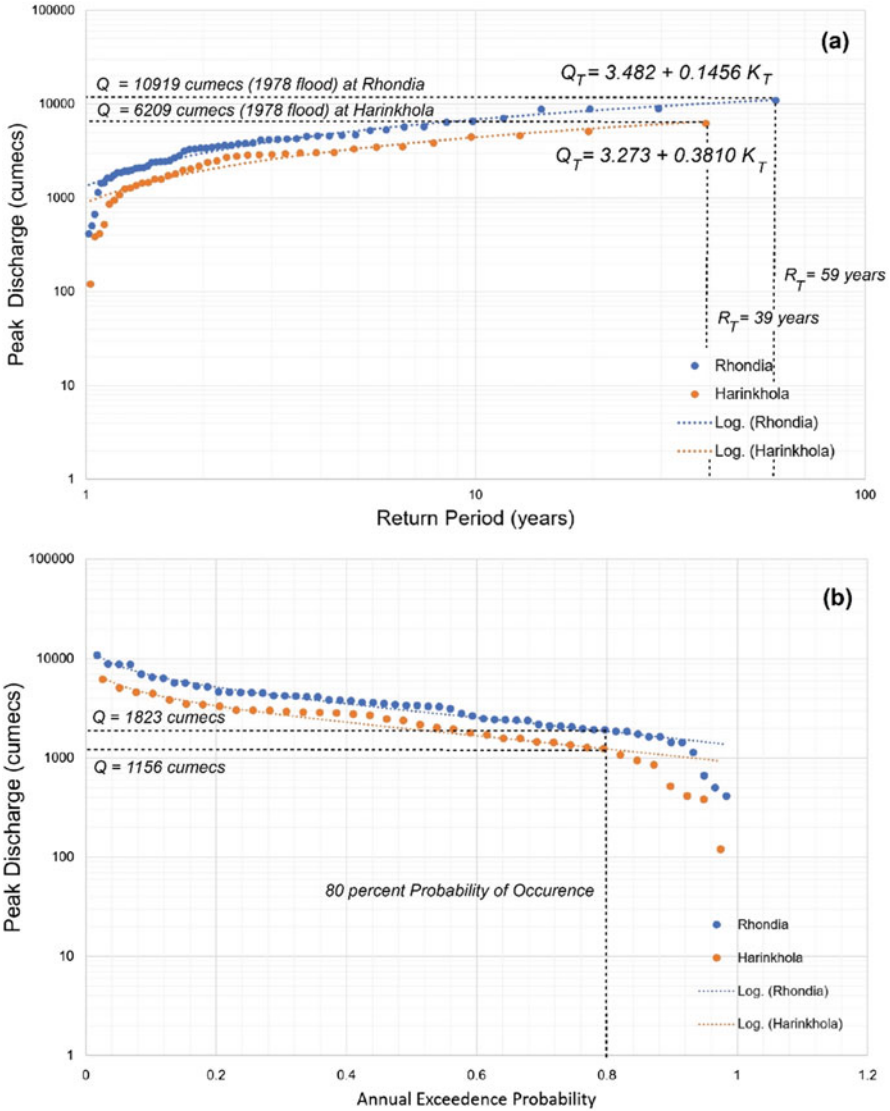


Fig. 13.11 (a) Dam-controlled LPT3 distributions of annual peak discharge in relation to return period at Rhondia (Damodar River) and at Harinkhola (Mundeswari River) and (b) comparative analysis of variability in annual exceedance probability of peak discharge at two river gauge stations

reason, the DVC had a prime objective to control the abnormal extreme flow under a critical level in the lower Damodar River.

4. The flood regulation system of DVC dams has turned the hydrological regime to a large extent. Now, a maximum flood flow of $10,919 \text{ m}^3\text{s}^{-1}$ has R_T of 59 years, and it has only 1.604% chance of being exceeded in any one year (Fig. 13.11a).

At present, annual peak discharge of 1443–1434 m^3s^{-1} has 1.11–1.09 years R_T , and it has 89–91% chance of occurrence in any one year. The 100-year flood of post-dam period is estimated about 11,969 m^3s^{-1} (reduction of 37.06% from the pre-dam 100-year flood flow), which has only 1% chance of occurrence in one of given year (i.e., 1 in 100 years). The 2-year flood (50% probability of occurrence) is estimated about 3234 m^3s^{-1} , (reduction of 58.44% from the pre-dam 2-year flood flow).

5. FFA at Harinkhola gauge station (1978–2015) reflects the extreme downstream flood flow condition of the Mundeswari River (western bifurcated channel of main Damodar River). The 100-year flood at this station is near about 8058 m^3s^{-1} , and the estimated 2-year flood is 2045 m^3s^{-1} . The observed maximum flood flow is 6208 m^3s^{-1} (observed in 1978) which has 39 years R_T , having 2.6% chance of occurrence in one of the given years. It is observed that there is 80% probability to encounter peak discharge of 1156–1183 m^3s^{-1} in the lower Damodar River (Fig. 13.11b).

5.4 1D Flood Simulation of Unsteady and Steady Flow

“Steady flow” refers to conditions that do not change with time. Mathematically, steady flow implies that $(\partial h/\partial t) = 0$, $(\partial V/\partial t) = 0$, and $(\partial Q/\partial t) = 0$. “Uniform flow” refers to conditions that do not change with space. Unsteady flow equations in open channels with friction define kinematic and dynamic waves. The model is performed on two bifurcated channels of the main Damodar River, viz., Mundeswari River and Damodar/Amta River (Fig. 13.12). In the first case, a database of unsteady flow (observed at Durgapur Barrage) is used in 1D flood simulation. A current low-magnitude flood wave (1410–1811 m^3s^{-1}) occurred during June 2021, and a hydrological simulation of discharge and gauge height was retrieved from IWD web database to understand the current flow regime at spatial scale in the platform of HEC-RAS 6.2 version. The hydrograph of early monsoon rainfall shows an escalation of base flow (nearer to 400 m^3s^{-1}) to 1811 m^3s^{-1} at a sudden due to release of excess water from the Durgapur Barrage (1 June–6 July 2021) (Fig. 13.13a). The unsteady flow got momentum from 18 June 2021 (846 m^3s^{-1}) and it reached peak on 22 June 2021, and then it gradually reduced to 487 m^3s^{-1} on 6 July 2021. A strong relationship between streamflow or daily discharge (Q_{un}) and station gauge height (G_h) was observed at Jamalpur and Champadanga gauge stations. With a high coefficient of determination, the stage-gauge height curve of Damodar River followed a power regression positive trend (Fig. 13.13b, c):

- At Jamalpur gauge station: $G_h = 9.4998 Q_{un}^{0.094}$
- At Champadanga gauge station: $G_h = 3.6743 Q_{un}^{0.1705}$

A flood management strategy is deduced from the empirical relationship. From this relationship an estimate of bankfull discharge (critical flow level for downstream

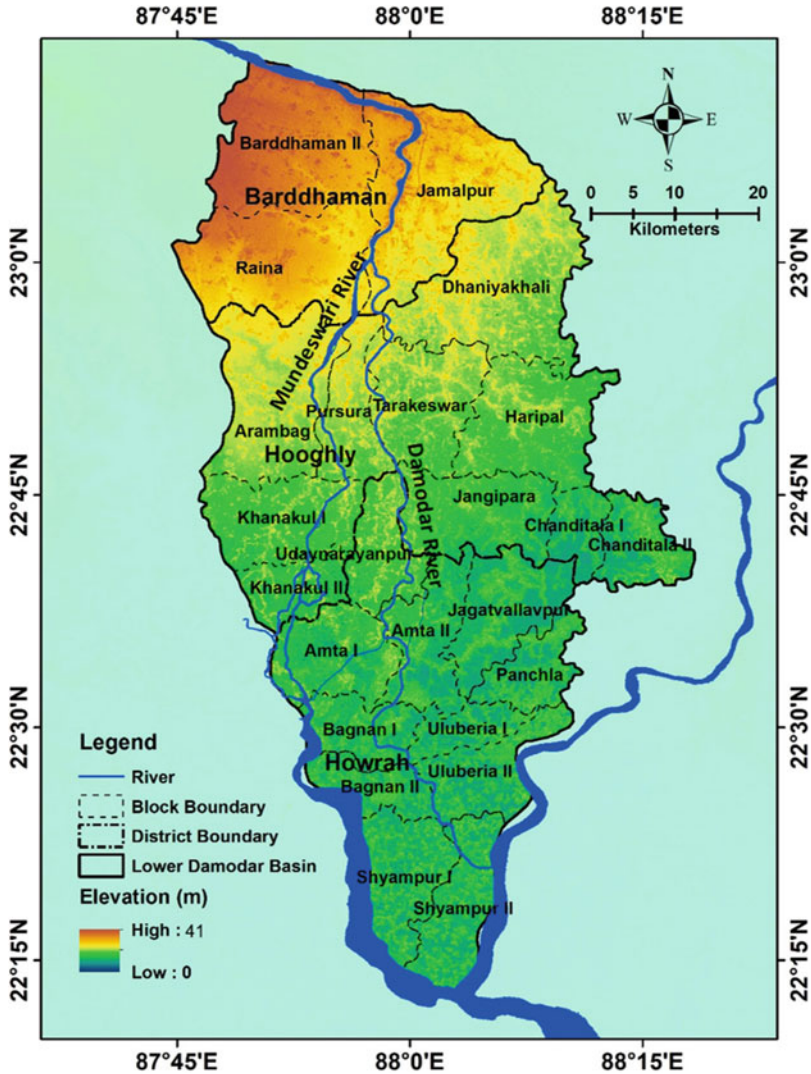


Fig. 13.12 Flood prone channels of lower Damodar River Basin (considered in HEC-RAS 1D hydrodynamic model) on the terrain of 0–41 m elevation, covering the administrative blocks of Purba Bardhaman, Hooghly, and Howrah districts (West Bengal)

inundation or overbank flow) can be established on the basis of danger level (DL) and extreme danger level (EDL) gauge heights at two stations. Alongside, the estimated bankfull discharge (Q_{bank}) reflects the present carrying capacity of channel (Table 13.7). Jamalpur gauge station is a vital location for flood prediction because from this site the main river is bifurcated into Munderwari channel and Damodar/Amda channel. At this site, Q_{bank} of DL (23.24 m from msl) and EDL

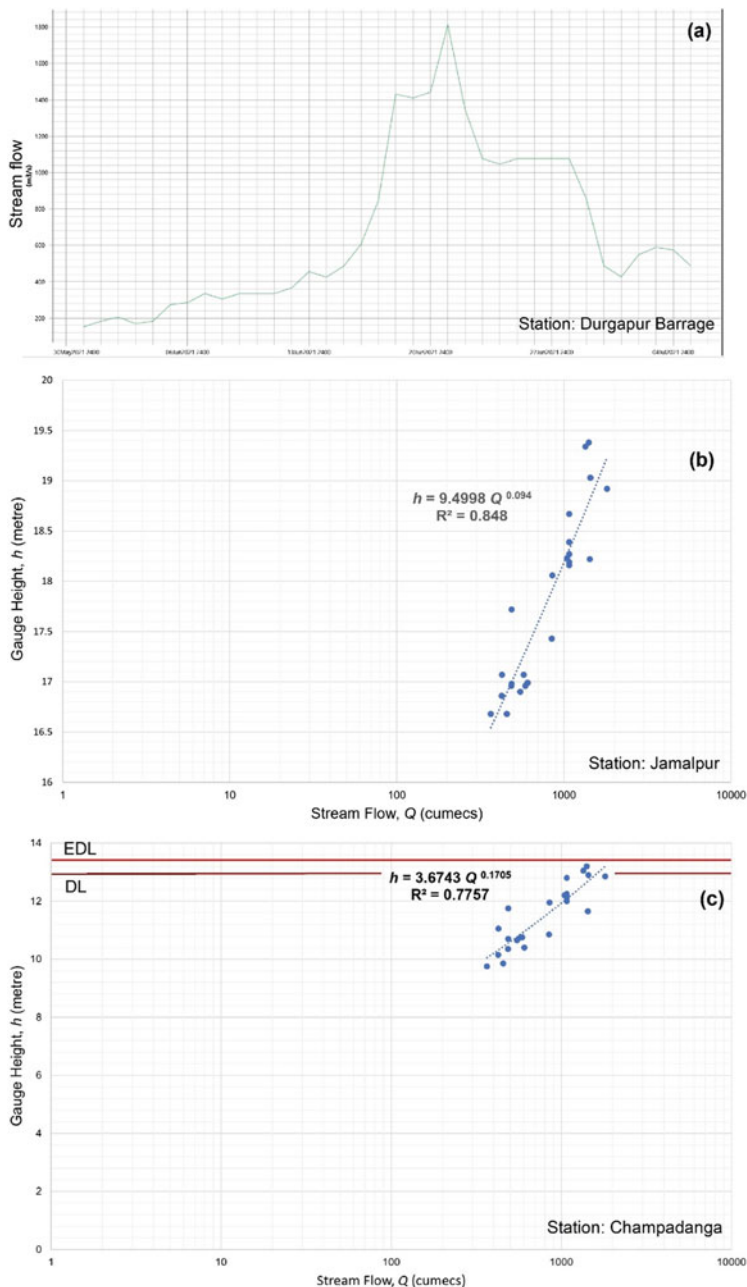


Fig. 13.13 (a) Schematic hydrograph of period 1 June–6 July 2021 observed at the Durgapur Barrage, (b) stage-streamflow rating curve at Jamalpur gauge station, and (c) stage-streamflow rating curve at Champadanga gauge station

Table 13.7 HEC-RAS estimated present critical bankfull discharge in the Mundeswari and Damodar channel

Parameters	Jamalpur gauge station	Champadanga gauge station	Harinkhola gauge station
Danger level (DL)	23.24 m	12.9 m	12.8 m
Extreme danger level (EDL)	23.54 m	13.5 m	13.41 m
Bankfull discharge at DL	$3198 \text{ m}^3\text{s}^{-1}$	$1353 \text{ m}^3\text{s}^{-1}$	$1518 \text{ m}^3\text{s}^{-1}$
Bankfull discharge at EDL	$3326 \text{ m}^3\text{s}^{-1}$	$1651 \text{ m}^3\text{s}^{-1}$	$1822 \text{ m}^3\text{s}^{-1}$

Note: Elevation of DL or EDL measured from mean sea level

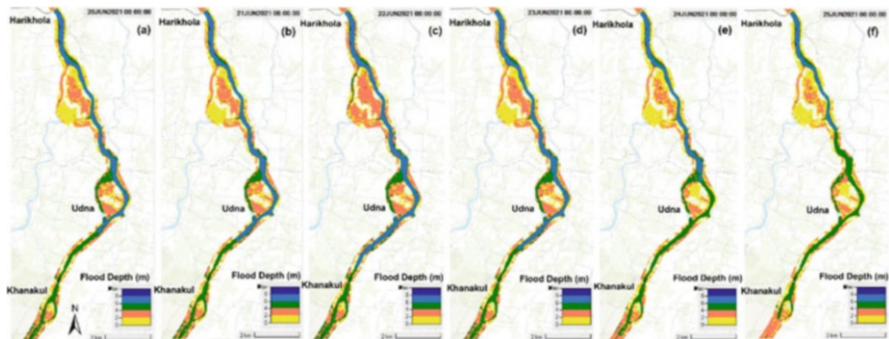


Fig. 13.14 HEC-RAS 1D floodplain inundation modelling output maps (a–f) of Mundeswari River (between Harinkhola and Khanakul) based on unsteady flow simulation (20–25 June 2021), noticing observed maximum discharge ($1811 \text{ m}^3\text{s}^{-1}$) on 22nd June, 2021

(23.54 m from msl) are $3198 \text{ m}^3\text{s}^{-1}$ and $3326 \text{ m}^3\text{s}^{-1}$, respectively. The peak flow at Champadanga gauge station determines the flood condition of Hooghly and Howrah districts. At this site, Q_{bank} of DL (12.9 m from msl) and EDL (13.5 m from msl) are $1353 \text{ m}^3\text{s}^{-1}$ and $1651 \text{ m}^3\text{s}^{-1}$, respectively. So, from this critical bankfull flow database, the DVC and IWD should regulate the flood flow or peak discharge (maintaining flow under critical level) to save the floodplains from a long period of inundation. During the unsteady flow of June–July 2021 the streamflow did not cross the bank at Jamalpur, but it overtopped the bank DL from 20–24 June 2021 ($>1410 \text{ m}^3\text{s}^{-1}$) at Champadanga, signifying the low carrying capacity of Amta channel and downstream vulnerability of flood.

1D flood simulation of HEC-RAS exhibits the floodplain inundation depths during a period of unsteady flow at downstream of Harinkhola gauge station ($22^\circ 50'22.38'' \text{ N}$, $87^\circ 54'15.75'' \text{ E}$). From the maps (Fig. 13.14) it is observed that in the floodplain of Mundeswari, the maximum flood depth of certain discharge (20–25 June 2021) varies from 1 to 8 m in the active channel area and the adjoining floodplain. On 22 June 2021 the region around Harinkhola, Udna, and Khanakul experienced inundation depth of greater than 3 m for the discharge of $1811 \text{ m}^3\text{s}^{-1}$

Table 13.8 HEC-RAS derived hydrologic statistics (unsteady flow) of the cross-sections along Mundeswari River and Damodar/Amta River

Hydrologic parameters	Mundeswari River		Damodar/Amta River	
	Upstream cross-section	Downstream cross-section	Upstream cross-section	Downstream cross-section
Total flow in channel area	1685.02 m ³ s ⁻¹	1457.07 m ³ s ⁻¹	1378.12 m ³ s ⁻¹	1081.22 m ³ s ⁻¹
Flow area	1056.88 m ²	548.11 m ²	687.86 m ²	478.91 m ²
EG elevation	18.78 m	14.69 m	18.45 m	16.13 m
WS elevation	18.65 m	14.35 m	18.28 m	15.91 m
EG slope	0.00440 m m ⁻¹	0.002270 m m ⁻¹	0.000471 m m ⁻¹	0.000750 m m ⁻¹
Minimum main channel elevation	13.00 m	9.00 m	12.00 m	11.00 m
Top width	199.2 m	163.14 m	268.97 m	214.92 m
Average velocity	1.55 m s ⁻¹	2.66 m s ⁻¹	1.68 m s ⁻¹	1.99 m s ⁻¹
Hydraulic depth in channel	5.31 m	3.36 m	5.81 m	4.91 m
Wetted perimeter	199.35 m	164.43 m	118.50 m	97.68 m
Shear	22.87 N m ⁻²	74.26 N m ⁻²	26.83 N m ⁻²	81.37 N m ⁻²
Stream power	36.47 N m s ⁻¹	197.29 N m s ⁻¹	53.75 N m s ⁻¹	36.47 N m s ⁻¹
Froude number	0.214	0.461	0.221	0.285

EG energy grade, WS water surface

which had crossed the bankfull discharge of DL and EDL (Table 13.5). The most critical level of bankfull discharge is 1518 m³s⁻¹ at downstream of Harinkhola. The hydrological estimates of downstream and upstream cross-sections reveal in Table 13.8. At upstream cross-section near Gotan, the channel can accommodate maximum flow of 1685 m³s⁻¹ and the flow area is 1057 m², but at downstream cross-section near Khanakul region, the flow area is reduced to 548.11 m² (48.15% reduction from upstream), and total flow along cross-section is maximum 1457 m³s⁻¹ (13.53% reduction from upstream). Energy grade slope of downstream cross-section is 0.002270 m m⁻¹ which is nearer to 0.00440 m m⁻¹ at upstream (almost double than downstream). For the certain maximum flow, the downstream stream power can reach up to 197.29 N m s⁻¹ (velocity of 2.66 m s⁻¹), having shear stress of 74.26 N m⁻², but it is relatively smaller in the case of upstream. The Froude number (F_r) of two cross-sections (0.214–0.461) exhibits subcritical flow of lower energy state (slow/tranquil flow regime) during the observed flood event.

In the steady flow 1D flood modelling the post-dam LPT3 designed potential discharges of 2-year R_T flood (3254 m³s⁻¹), 5-year R_T flood (5324 m³s⁻¹), 10-year R_T flood (6676 m³s⁻¹), and 25-year R_T flood (8292 m³s⁻¹) are taken into consideration to observe the spatial extent of floodplain inundation along the Mundeswari River. From the maps (Fig. 13.15) it is observed that maximum part of active channel area (38.84 km) can experience a flood depth of 4–8 m in 2-year flood, with floodplain inundation depth of less than 4 m at some parts of Khanakul. During

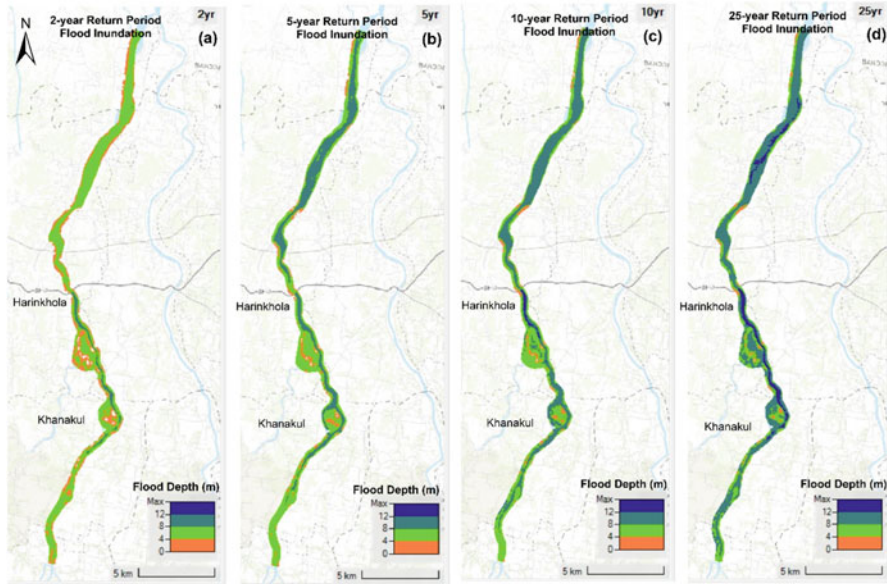


Fig. 13.15 HEC-RAS 1D model derived potential floodplain inundation maps (a–d) of Mundeswari River based on steady flow simulation (LPT3 distribution designed 2-year, 5-year, 10-year, and 25-year flood discharge), noticing flood depth of over 12 m during 25-year flood of $8292 \text{ m}^3\text{s}^{-1}$

5-year and 10-year flood event, the depth can reach 4–12 m from the bifurcation point to Khanakul, and it has maximum chance of overbank flow crossing the embankments of Khanakul region. In a 25-year flood, the total channel and active floodplain area can experience flood depth of beyond 8 m, and in between Harinkhola and Khanakul, the depth can exceed 12 m, recognizing the critical site of embankment failure and flood vulnerability (exceeding EDL and EDL).

In the 1D flood model of unsteady flow, the downstream section (Damodar/Amta channel) of Champadanga gauge station ($22^{\circ}50'22.92'' \text{ N}$, $87^{\circ}58'11.75'' \text{ E}$) shows marked variation of flood depths (1–8 m) for the streamflow simulation during 1 June–6 July 2021. On 20 June, 2021, due to flow rate of $1410 \text{ m}^3\text{s}^{-1}$, the flood depth varied from 1 to 4 m below Udaynarayan region, and the active channel part experienced greater than 6 m deep water (Fig. 13.16). On 22nd June, 2021 the flow rate reached up to $1811 \text{ m}^3\text{s}^{-1}$ and the flood depth exceeded 6 m near Rajbalhat region, and at the downstream of Udaynarayanpur, the depth touched 2–6 m range, across the embanked floodplain. The observed discharge from 20th to 25th June, 2021 had crossed the bankfull limit of DL and EDI (Table 13.5), and the vast region of Joynagar and Udaynaryanpur was flooded. At upstream cross-section near Jamdara, the channel can accommodate maximum flow of $1378 \text{ m}^3\text{s}^{-1}$ and the flow area is 687 m^2 , but at downstream cross-section near Udaynarayanpur region, the flow area is recued to 478 m^2 (30.42% reduction from upstream), and total flow along cross-section is maximum $1081 \text{ m}^3\text{s}^{-1}$ (21.55% reduction from upstream)

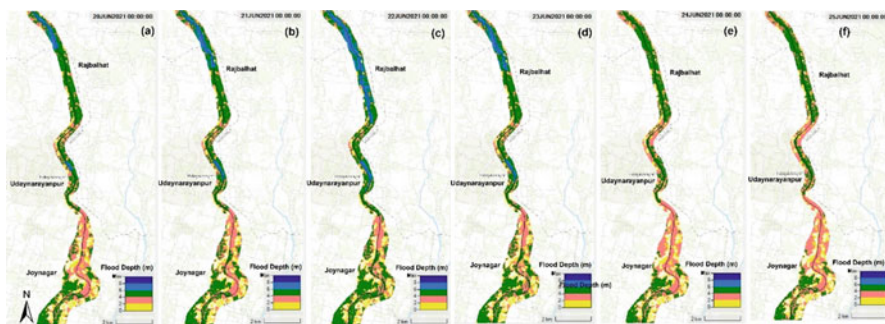


Fig. 13.16 Thematic flood depth maps (a–f) of Damodar/Amta Channel (between Rajbalhat and Udaynaryanpur) using HEC-RAS 1D floodplain inundation modelling on unsteady flow simulation (20th–25th June, 2021)

(Table 13.6). Energy grade slope of downstream cross-section is $0.000471 \text{ m m}^{-1}$ which is nearer to $0.000750 \text{ m m}^{-1}$ at upstream. The downstream stream power can reach up to 81.37 N m s^{-1} (velocity of 1.99 m s^{-1}), having shear stress of 36.47 N m^{-2} , but it is relatively higher in case of upstream. The Froude number (F_r) of two cross-sections (0.221–0.285) exhibits subcritical flow of lower energy state during the observed flood event of 1st June–6th July, 2021.

In steady flow 1D hydrodynamic model, the Damodar/Amta channel (49.26 m stretch) can experience devastating flood because all LPT3-designed potential discharges of 2-year, 5-year, 10-year, and 25-year flood can exceed the bankfull limit of Champadanga gauge station (Fig. 13.17). In a 2-year flood ($3254 \text{ m}^3 \text{ s}^{-1}$), the maximum floodplain inundation depth can range from 6 to 8 m from the bifurcation point to Udaynaryanpur. During 5-year and 10-year floods, the depth of flood water can exceed 8 m at downstream of Champadanga. The flood depth can reach beyond 10 m during a 25-year flood along the 34.40 km stretch of Damodar channel. The most vulnerable site of embankment failure and overbank flow is stretch between Rajbalhat and Udaynaryanpur where the flood depth can cross 10 m limit for the discharge of $1811 \text{ m}^3 \text{ s}^{-1}$.

6 Discussion

The DVC has now completed 75 years in 2022, and the authority has experienced a number of success (mainly irrigation water supply and flood control) as well as failure (mainly river metamorphosis and downstream recurrent flood), but it is worthwhile to mention that the prime objective of DVC was to make the Damodar Valley as an Eden of economic potentiality or “Valles Opima” of India (Kirk, 1950) which was partly achieved. The DVC dams and flood regulation system are now not able to manage sudden peak monsoonal flow to save the floodplains of lower DRB (mainly Purba Bardhaman, Hooghly, and Howrah districts). During late monsoon

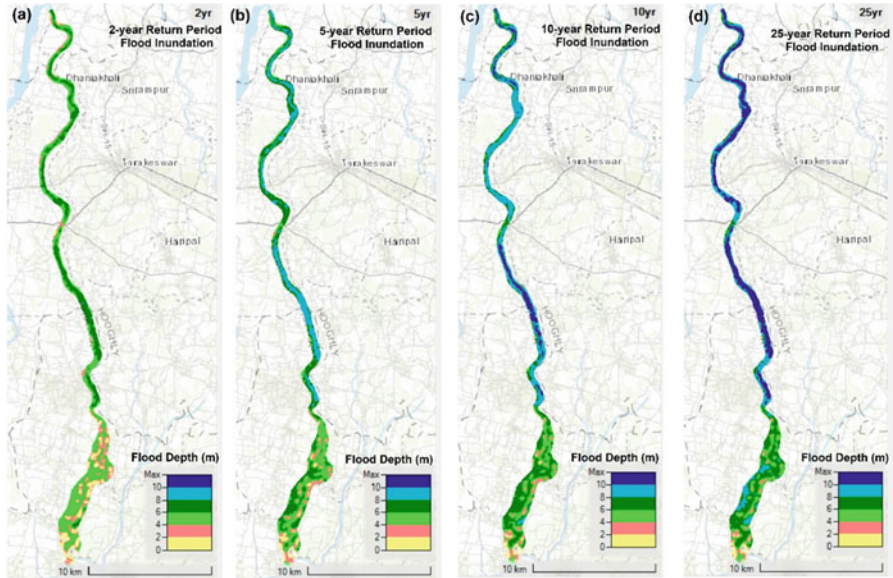


Fig. 13.17 HEC-RAS 1D model derived potential floodplain inundation maps (a–d) of Damodar/Amta Channel based on steady flow simulation (LPT3 distribution designed 2-year, 5-year, 10-year, and 25-year flood discharge), observing flood depth of greater than 12 m during a 25-year flood ($8292 \text{ m}^3\text{s}^{-1}$)

consecutive torrential rainfall from the tropical depressions or cyclones, the last two terminal dams, Panchet and Maithon, are compelled to release excess water (less capacity of flood storage due to siltation) which recurrently turns into nightmare for the inhabitants of the Damodar fan-delta floodplains. The funnel-shaped basin size, with a wide upper catchment and a narrow bottle-neck location at downstream, has potentiality of phenomenal increase in peak discharge in the lower Damodar River. The DVC dams have successfully reduced the flood heights, i.e., furious peak discharge of greater than $12,000 \text{ m}^3\text{s}^{-1}$ with short duration, but now the flood peaks are decreased significantly, except flood of September, 1978 ($10,919 \text{ m}^3\text{s}^{-1}$), and the duration of inundation period becomes large. Preliminary report suggested to build eight large dams to moderate maximum peak discharge of $28,000 \text{ m}^3\text{s}^{-1}$ – $7079 \text{ m}^3\text{s}^{-1}$ at Rhondia gauge station, but now five dams (including Tenughat Dam) only provide flood storage of 3591 million m^3 which was only 55% of storage capacity as mentioned in the report. Therefore, the present flood regulation system of DVC does not have full capability to regulate exceptional peak discharge of 100-year flood ($11,969 \text{ m}^3\text{s}^{-1}$).

In the trans-Damodar area of fan-delta (i.e., Late Quaternary – Recent floodplains of Mundeswari and Amta channels), the floods are encountered in each year, and it is mainly caused by the drainage congestion in the channels, tidal influence at outlet, and increasing siltation which promotes reduction of flow area in the active channel part. Hydrometeorological observations exhibit that in late monsoon month

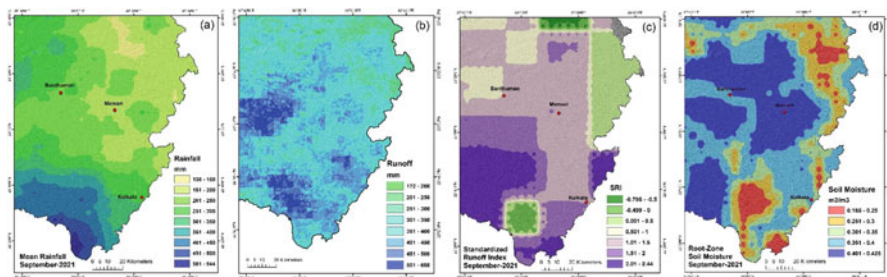


Fig. 13.18 Hydrometeorological maps of the Damodar fan-delta (covering floodplains of Mundeswari and Damodar/Amta channel) – (a) spatial concentration of monsoon rainfall (September 2021), (b) mean runoff potential of monsoon months based on NRCS-CN method, (c) Standard Runoff Index (SRI) map of September 2021 (SRI > 0 means surplus runoff water) and (d) Root-Zone Soil Moisture map of September 2021 (RZSM > 0.40 means excess soil moisture)

(September–October, 2021), the fan-delta region receives more than 251 mm monthly rainfall, reaching high root zone moisture at maximum level ($0.351\text{--}0.425\text{ m}^3/\text{m}^3$) and high standardized runoff index ($1.51\text{--}2.44$) in the active floodplains (Fig. 13.18). During that time, the region does not capacity to absorb excessive water coming from high flood discharge (due to 3–4 days rainstorm in the upper catchment), and then, the inundation of floodplains for longer period was an inevitable condition. In addition, the Quaternary floodplains of Damodar fan-delta region have high potentiality of surface runoff in a range of 172–608 mm during the monsoon months, and the free flow is hampered due to tidal inflow from the Bhagirathi-Hooghly River. The miserable flood situation is aggravated by adding of excess water from the DVC canals by breaches, tail discharge, and over toping. The further analysis suggests some following suggestions to improve the flood management strategies of DRB:

- Intense short spells (usually 3–4 days) of extreme rainfall ($150\text{--}290\text{ mm}$) are now very common in each year due to aggravation of extreme climatic events in response to global climate change. A rainstorm magnitude equal to or greater than 304.8 mm may occur once in 100 years. This study has estimated the probable maximum rainfall for a given magnitude of flood: (a) 2-year flood ($3254\text{ m}^3\text{s}^{-1}$) rainfall, 205 mm; (b) 10-year flood ($6676\text{ m}^3\text{s}^{-1}$) rainfall, 304 mm; (c) 50-year flood ($9417\text{ m}^3\text{s}^{-1}$) rainfall, 360 mm; and (d) 100-year flood ($11,969\text{ m}^3\text{s}^{-1}$) rainfall, 412 mm. Therefore, from the early precise prediction of heavy rainfall (now given by Indian Meteorological Department), the DVC authority can regulate the flows in all reservoirs to reduce the peak flow under $7079\text{ m}^3\text{s}^{-1}$ at Rhondia or at the Durgapur Barrage. In this case, a good coordination between DVC and IWD is needed to act on real-time flood forecast for the sake of inhabitants living in the low-lying floodplains of Hooghly and Howrah districts.
- Reduction of reservoirs' flood storage capacity, due to excessive siltation, is another problem in the DRB. The Maithon and Panchet reservoirs have lost

significant amount of overall storage capacity, viz., 27.4% in Maithon and 15.9% in Panchet, respectively. The sedimentation rates of the reservoirs are depicted as follows: (a) Konar, $1748 \text{ m}^3 \text{ km}^{-2} \text{ year}^{-1}$; (b) Maithon, $1076 \text{ m}^3 \text{ km}^{-2} \text{ year}^{-1}$; (c) Panchet, $631 \text{ m}^3 \text{ km}^{-2} \text{ year}^{-1}$; (d) Tenughat, $716 \text{ m}^3 \text{ km}^{-2} \text{ year}^{-1}$; and (e) Tilaiya, $2792 \text{ m}^3 \text{ km}^{-2} \text{ year}^{-1}$ (Ghosh et al., 2022a). The sedimentation rate can be managed by installing small check dams in the gullies or streams of upper catchments. Regular dredging of the reservoirs is very much needed to increase the functional longevity of dams and to check flood risk.

- HEC-RAS 1D hydrodynamic model reveals that present carrying capacity (i.e., critical limit of overbank flow) of Mundeswari and Damodar/Amta channel is near about $1518\text{--}1822 \text{ m}^3 \text{ s}^{-1}$ and $1353\text{--}1651 \text{ m}^3 \text{ s}^{-1}$, respectively. It is predicted the floodplain inundation region (flood depth of 1–12 m) in respect to 2-year, 5-year, 10-year, and 25-year flood. The most vulnerable sites of embankment failure and overbank flow are the 27 km long Damodar/Amta channel from Rajbalhat to Udaynarayanpur and 19 km long Mundeswari channel from Udna to Khanakul. If the HEC-RAS 1D model database is calibrated and validated with actual field result or SAR (synthetic aperture radar) flood dataset, the floodplain inundation prediction can be done precisely for a certain streamflow in the river valleys of Hooghly and Howrah districts.
- Finally, the Damdoar fan-delta region should be saved from drainage congestion during the monsoon months. Construction of marginal embankments, settlements, railways, and dense network of roads have aggravated the miserable flood situation (Fig. 13.19a). Embankments serve the purpose of preventions of floods for the time being but tend to create more problems later. Behind the embankments vested interests grow up encroaching into the active floodplain of the river. Development of additional settlements, roads, and cropland, around the active floodplains, hinders the flow paths of overbank discharge, and it transforms the palaeochannels of Damodar to abandoned channels permanently. It is suggested that if the palaeochannels or abandoned channels are linked with main river, Mundeswari and Damodar/Amta, through sluice gates, then the peak monsoon flow can be distributed along those channels during floods to reduce the rate of peak discharge in main river (downstream of Harinkhola and Champadanga) and to save the low-lying floodplains from recurrent inundation (Fig. 13.19b).

7 Conclusion

Seven decades (completed 75 years) have passed since the partial implementation of the DVC project. The life span of the reservoirs is also coming to an end, and the effectiveness of flood-controlling system is declining. The benefit that was found in the first episode, the level of evil in the next episode is surpassing the inhabitants of lower Damodar valley. The DVC should start to think about the alternative plan to mitigate excess streamflow through construction of another dam or preparation of

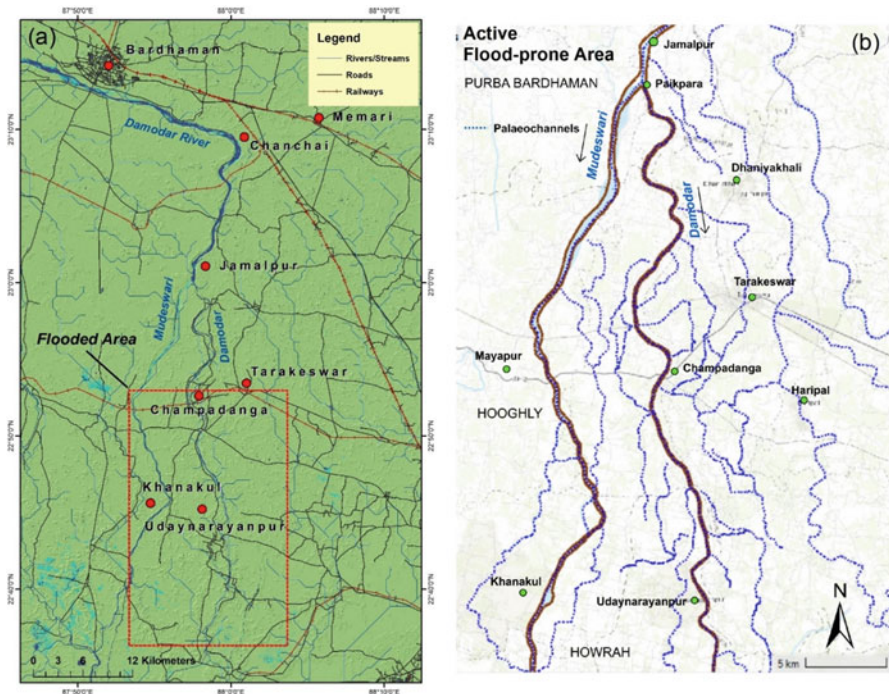


Fig. 13.19 (a) Dense network of roads and railways in the floodplain of Damodar fan-delta region, promoting drainage congestion and (b) downstream palaeochannels and abandoned channels of Mundeswari and Damodar/Amta channel, having the option of reconnecting with the main river through sluice gates

numerous check dams at upstream. The need of dredging is an immediate task to extend the life span of reservoirs. Alongside the IWD should maintain coordination with DVC during the release of flood water. Alternatively, IWD may think about the rejuvenation of palaeochannels, connecting the old and abandoned courses of Damodar and Mundeswari with the main channel for evenly distribution of the excess streamflow during flood. The current study provides an outlook on the probable maximum rainfall in connection with expected flood discharge and the spatial dimension of the floodplain inundation model, which can be applied to reduce flood risk. The future research need to develop a real-time geospatial model of rainfall – streamflow simulation to predict peak discharge for a certain rainfall and the probable region of inundation or overbank flow. Another application of 1D/2D hydrodynamic model is now needed to calculate the flooded areas of different land use categories for estimating the monetary loss and economic vulnerability.

References

- Acharyya, S. K., & Shah, B. A. (2007). Arsenic-contaminated groundwater from parts of Damodar fan-delta and west of Bhagirathi River, West Bengal, India: Influence of fluvial geomorphology and Quaternary morphostratigraphy. *Environmental Geology*, 52, 489–501. <https://doi.org/10.1007/s00254-006-0482-z>
- Albano, R., Mancusi, L., Sole, A., & Adamowski, J. (2017). Flood risk: A collaborative, free and open-source software for flood risk analysis. *Geomatics, Natural Hazards and Risk*, 8(2), 1812–1832. <https://doi.org/10.1080/19475705.2017.1388854>
- Bagchi, K. G. (1977). The Damodar Valley and its impact on the region. In A. G. Noble & A. Rudra (Eds.), *Indian urbanization and planning: Vehicles of modernization*. Tata McGraw-Hill Publishing Co. Ltd.
- Baker, V. R. (1994). Geomorphological understanding of floods. *Geomorphology*, 10, 139–156.
- Bera, S., & Mistri, B. (2014). Flood in the lower Damodar Basin and channel morphology: A case study at the bifurcation zone into Damodar and Mundeswari River, West Bengal. *International Journal of Geology, Earth and Environmental Sciences*, 4(2), 172–181.
- Betscholtz, A., & Nordlof, B. (2017). *Potentials and limitations of 1D, 2D and coupled 1D-2D flood modelling in HEC-RAS*. Division of Water Resource Engineering, Lund University. <https://lup.lub.lu.se/student-papers/record/8904721/file/8904723.pdf>
- Bhalla, D. N. (1969). The Damodar Valley Corporation: A study of the transplantation of foreign administrative institutions into India. Doctoral thesis, Radboud University Nijmegen. <https://repository.ubn.ru.nl/handle/2066/148493>
- Bhattacharya, K. (2011). *The Lower Damodar River, India: Understanding the Human Role in Changing Fluvial Environment*. Springer, Dordrecht. <https://doi.org/10.1007/978-94-007-0467-1>.
- Burn, D. H., Castellarin, A., & Kjeldsen, T. R. (2017). Floods. In V. P. Singh (Ed.), *Handbook of applied hydrology* (pp. 75-1–75-7). McGraw Hill.
- Chandra, S. (2003). *Integrated flood management case study India: Flood management – Damodar River Basin*. WMO/GWP Associated Programme on Flood Management. http://www.floodmanagement.info/publications/casestudies/cs_india_full.pdf
- Chatterjee, S. P. (1967). *Damodar Valley planning Atlas*. NATMO.
- Chatterjee, S. P. (1969). *The planning atlas of the amodar Valley region*. International Geological Congress, Calcutta
- Chattopadhyay, S., Acharya, R., & Sen, A. K. (2020). Analysis of rainfall trends in Damodar valley area. *VayuMandal*, 46(2), 61–72.
- Choudhury, S. (2012). Damodar Valley Corporation, the missed opportunity. *Journal of Infra-structural Development*, 3(2), 117–226. <https://doi.org/10.1177/097493061100300202>
- Climate Signals. (2022). *Atmospheric moisture increase*. <https://www.climate-signals.org/climate-signals/atmospheric-moisture-increase#:~:text=A%20warmer%20atmosphere%20holds%20more,mores%20moisture%20as%20it%20warms>
- Correia, F. N., Rego, F. C., Saraiva, M. D. G., & Ramos, I. (1998). Coupling GIS with hydrologic and hydraulic flood modelling. *Water Resources Management*, 12, 229–249.
- Das, B., Pal, S. C., & Malik, S. (2017). Assessment of flood hazard in a riverine tract between Damodar and Dwarkeswar River, Hugli District, West Bengal, India. *Spatial Information Research*, 26, 91–101.
- Dasallas, L., Kim, Y., & An, H. (2019). Case study of HEC-RAS 1D-2D coupling simulation: 2002 Baeksan flood event in Korea. *Water*, 11, 2048. <https://doi.org/10.3390/w11102048>
- De Saint Venant, B. (1871). Theorie du mouvement non-permanent ´ des eaux avec application aux crues des rivieres et a l’introduction des marees dans leur lit. *Comptes Rendus de l’Acad’emie des Sciences*, 73, 148–154, 237–240.
- Fan, Y., Ao, T., Yu, H., Huang, G., & Li, X. (2017). A coupled 1D-2D hydrodynamic model for urban flood inundation. *Advances in Meteorology*, 2017, Article ID 2819308. <https://doi.org/10.1155/2017/2819308Advncns>

- Farooq, M., Shafique, M., & Khattak, M. S. (2019). Flood hazard assessment and mapping of River Swat using HEC-RAS 2D model and high-resolution 12-m TanDEM-X DEM (World DEM). *Natural Hazards*, 97, 477–492.
- Garde, R. J. (2006). *River morphology*. New Age International.
- Ghosh, S. (2011). Hydrological changes and their impact on fluvial environment of the lower Damodar Basin over a period of fifty years of damming The Mighty Damodar River in Eastern India. *Procedia – Social and Behavioral Sciences*, 19, 511–519.
- Ghosh, S. (2013). *Flood hydrology and risk assessment: Flood study in a dam-controlled river of India*. Lambert Academic Publishing.
- Ghosh, S., & Guchhait, S. K. (2015). Characterization and evolution of primary and secondary laterites in northwestern Bengal Basin, West Bengal, India. *Journal of Palaeogeography*, 4(2), 203–230. <https://doi.org/10.3724/SP.J.1261.2015.00074>
- Ghosh, S., & Guchhait, S. K. (2016). Dam-induced changes in flood hydrology and flood frequency of tropical river: A study in Damodar River of West Bengal, India. *Arabian Journal of Geosciences*, 9(2), 1–26. <https://doi.org/10.1007/s12517-015-2046-6>
- Ghosh, S., & Illahi, A. (2020). Responses of fluvial forms and processes to human actions in the Damodar River Basin. In B. Das et al. (Eds.), *Anthropogeomorphology of Bhagirathi-Hooghly River system in India* (pp. 213–251). CRC Press.
- Ghosh, S., & Mistri, B. (2015). Geographic concerns on flood climate and flood hydrology in monsoon-dominated Damodar River Basin, Eastern India. *Geography Journal*, 2015, 1. <https://doi.org/10.1155/2015/486740>
- Ghosh, P. K., Mukhopadhyay, R., & Jana, N. C. (2021). Quantitative analysis of drainage basin parameters towards better management of Damodar River, Eastern India. *Journal Geological Society of India*, 97, 711–734.
- Ghosh, S., Hoque, M. M., Saha, U. D., & Islam, A. (2022a). Assessment of dam-induced changes in ecogeomorphological behaviour and fluvial functionality in the Damodar River, West Bengal, India. *Journal of Water Supply: Research and Technology-Aqua*, 71, 722. <https://doi.org/10.2166/aqua.2022.003>
- Ghosh, A., Roy, M. B., & Roy, P. K. (2022b). Evaluating the performance of MIKE NAM model on rainfall-runoff in lower Gangetic floodplain, West Bengal, India. *Modelling Earth Systems and Environment*, 168, 4001. <https://doi.org/10.1007/s40808-021-01347-6>
- Gibson, S., Pak, J., & Fleming, M. (2010, August 23–27). *Modeling watershed and riverine sediment processes with HEC-HMS and HEC-RAS*. Watershed Management Conference. [https://doi.org/10.1061/41143\(394\)120](https://doi.org/10.1061/41143(394)120)
- Glass, E. L. (1924). Floods of the Damodar River and rainstorms producing them. *Minutes Proc*, 217, 333–346.
- Goodarzi, M., & Eslamain, S. (2022). Riverine and flood modeling software. In S. Eslamain & F. Eslamain (Eds.), *Flood handbook analysis and modelling* (pp. 353–368). CRC Press.
- Goodell, C. R. (2005, May 15–19). *Dam break modeling for tandem reservoirs—A case study using HEC-RAS and HEC-HMS*. World Water and Environmental Resources Congress. [https://doi.org/10.1061/40792\(173\)402](https://doi.org/10.1061/40792(173)402)
- Hall, J. W., & Penning-Rosewell, E. C. (2011). Setting the scene for flood risk management. In J. W. Hall & E. C. Penning-Rosewell (Eds.), *Flood risk science and management* (pp. 3–16). Wiley. <https://doi.org/10.1002/9781444324846.ch1>
- Hayden, B. P. (1988). Flood climates. In V. R. Baker, R. C. Kochel, & P. C. Patton (Eds.), *Flood geomorphology* (pp. 13–27). Wiley.
- Hicks, F. E., & Peacock, T. (2005). Suitability of HEC-RAS for flood forecasting. *Canadian Water Resources Journal*, 30(2), 159–174. <https://doi.org/10.4296/cwrj3002159>
- Hirschboeck, K. K. (1988). Flood hydroclimatology. In V. R. Baker, R. C. Kochel, & P. C. Patton (Eds.), *Flood geomorphology* (pp. 27–50). Wiley.
- Hoque, M. M., Islam, A., & Ghosh, S. (2022). Environmental flow in the context of dams and development with special reference to the Damodar Valley Project, India: A review. *Sustainable Water Resources Management*, 8, 62. <https://doi.org/10.1007/s40899-022-00646-9>

- Horritt, M. S., & Bates, P. D. (2002). Evaluation of 1D and 2D numerical models for predicting river flood inundation. *Journal of Hydrology*, 268, 87–99.
- Hunter, W. W. (1876). *A statistical account of Bengal – Vol. 4*. Trubner & Co.
- Jagadesh, B., & Veni, K. K. (2021). Floodplain modelling of Krishna lower basin using ArcGIS, HEC-GeoRAS and HEC-RAS. *IOP Conference Series: Materials Science and Engineering*, 1112, 012024. <https://doi.org/10.1088/1757-899X/1112/1/012024>
- Kale, V. S. (2003). Geomorphic effects of floods in Indian Rivers. *Natural Hazards*, 28, 65–84.
- Kamal, N., & Pachauri, S. (2019). Mann-Kendall, and Sen's slope estimators for precipitation trend analysis in North-Eastern states of India. *International Journal of Computer Applications*, 177(11), 7–16.
- Karim, S., & De, S. K. (2019). Impact of dam on river discharge: A study on the Damodar River, Jharkhand. *Journal of Indian Geomorphology*, 6, 116–124.
- Khattak, M. S., Anwar, F., Saeed, T. V., Sharif, M., Sheraz, K., & Ahmed, A. (2016). Floodplain mapping using HEC-RAS and ArcGIS: A case study of Kabul River. *Arabian Journal for Science and Engineering*, 41, 1375–1390.
- Kinghton, D. (2014). *Fluvial forms and processes*. Routledge.
- Kirk, V. (1950). The Damodar Valley “Valles Opima”. *Geographical Review*, 40(3), 415–443. <https://doi.org/10.2307/211218>
- Knebl, M., Yang, Z. L., Hutchison, K., & Maidment, D. (2005). Regional scale flood modeling using NEXRAD rainfall, GIS, and HEC-HMS/RAS: A case study for the San Antonio River Basin Summer 2002 storm event. *Journal of Environmental Management*, 75(4), 325–336. <https://doi.org/10.1016/j.jenvman.2004.11.024>
- Kumar, N., Lal, D., Sherring, A., & Issac, R. K. (2017). Applicability of HEC-RAS and GFMS tool for 1D water surface elevation/flood modelling of the river: A case study of River Yamuna at Allahabad (Sangam), India. *Modelling Earth Systems and Environment*, 3, 1463–1475. <https://doi.org/10.1007/s40808-017-0390-0>
- Kumar, N., Kumar, M., Sherrig, A., Suryavanshi, S., Ahmad, A., & Lal, D. (2019). Applicability of HEC-RAS 2D and GFMS for flood extent mapping: A case study of Sangam area, Prayagraj, India. *Modelling Earth Systems and Environment*, 6, 397–405.
- Lahiri-Dutt, K. (2012). Large dams and changes in an agrarian society: Gendering the impacts of Damodar Valley Corporation in eastern India. *Water Alternatives*, 5(2), 529–542.
- Lahiri-Dutt, K., & Samanta, G. (2013). *Dancing with the river*. Yale University Press. <https://doi.org/10.12987/9780300189575>
- Leandro, J., Chen, A. S., Djordjević, S. & Savić, D. A. (2009). Comparison of 1D/1D and 1D/2D coupled (Sewer/Surface) hydraulic models for urban flood simulation. *Journal of Hydraulic Engineering* 135(6), 495–504. [https://doi.org/10.1061/\(ASCE\)HY.1943-7900.0000037](https://doi.org/10.1061/(ASCE)HY.1943-7900.0000037)
- Lee, K. T., Ho, Y. H., & Chyan, Y. J. (2006). Bridge blockage and overbank flow simulations using HEC-RAS in the Keelung River during the 2001 Nari typhoon. *Journal of Hydraulic Engineering*, 132(3), 319–323. [https://doi.org/10.1061/\(ASCE\)0733-9429\(2006\)132:3\(319\)](https://doi.org/10.1061/(ASCE)0733-9429(2006)132:3(319))
- Mahata, H. K., & Maiti, R. (2019). Evolution of Damodar fan delta in the western Bengal Basin, West Bengal. *Journal of Geological Society of India*, 93, 645–656.
- Mahata, H. K., & Maiti, R. (2020). Alluvial fan flooding in Lower Damodar Basin, West Bengal. *Geographical Review of India*, 82(1), 1–16.
- Majumder, M., Barman, R. N., Roy, P., Jana, B. K. & Mazumder, A. (2010a). Estimation of reservoir discharge with the help of clustered neurogenetic algorithm. In: Jana, B., Majumder, M. (eds) *Impact of climate change on natural resource management*. Springer, Dordrecht.
- Majumder, M., Roy, P., & Mazumdar, A. (2010b). An introduction and current trends of Damodar and Rupnarayan river system. In B. Jana & M. Majumder (Eds.), *Impact of climate change on natural resource management* (pp. 461–486). Springer.
- Malik, S., & Pal, S. C. (2021). Potential flood frequency analysis and susceptibility mapping using CMIP5 of MIROC5 and HEC-RAS model: A case study of lower Dwarkeswar River, Eastern India. *SN Applied Sciences*, 3, 31. <https://doi.org/10.1007/s42452-020-04104-z>

- Mandal, S. P., & Chakrabarty, A. (2016). Flash flood risk assessment for upper Teesta River basin: Using the hydrological modelling system (HEC-HMS) software. *Modeling Earth Systems and Environment*, 2, 59. <https://doi.org/10.1007/s40808-016-0110-1>
- Mawasha, T. S. (2021). Combined 1D modelling with HEC-RAS for delineation floodplain area: A case study of Hennops River in the Centurion Area. *American Journal of Mathematical and Computer Modelling*, 6(4), 55–62.
- Merwade, V., Olivera, F., Araabi, M., & Edleman, S. (2008). Uncertainty in flood inundation mapping: Current issues and future directions. *Journal of Hydraulic Engineering*, 13(7), 608. [https://doi.org/10.1061/\(ASCE\)1084-0699\(2008\)13:7\(608\)](https://doi.org/10.1061/(ASCE)1084-0699(2008)13:7(608))
- Mojaddadi, H., Pradhan, B., Nampak, H., Ahmad, N., & Ghazali, A. H. (2017). Ensemble machine-learning-based geospatial approach for flood risk assessment using multi-sensor remote sensing data and GIS. *Geomatics, Natural Hazards and Risk*, 8(2), 1080–1102.
- Nguyen, P., Shearer, E. J., Tran, H., Ombadi, M., Hayatbini, N., Palacios, T., Huynh, P., Braithwaite, D., Updegraff, G., Hsu, K., Kuligowski, B., Logan, W. S., & Sorooshian, S. (2019). The CHRS Data Portal, an easily accessible public repository for PERSIANN global satellite precipitation data. *Nature Scientific Data*, 6, Article number: 180296. <https://doi.org/10.1038/sdata.2018.296>
- Ogras, S., & Onen, F. (2020). Flood analysis with HEC-RAS: A case study of Tigris River. *Advances in Civil Engineering*, Article ID 6131982. <https://doi.org/10.1155/2020/6131982>
- Ongdas, N., Akiyanova, F., Karakulov, Y., Muratbayeva, A., & Zinabdin, N. (2020). Application of HEC-RAS (2D) for flood hazard maps generation for Yesil (Ishim) river in Kazakhstan. *Water*, 12, 2672. <https://doi.org/10.3390/w12102672>
- Parsa, A. S., Heydari, M., Sadeghian, M. S., & Moharrampour, M. (2013). Flood zoning simulation by HEC-RAS model (Case Study: Johor River-Kota Tinggi Region). *Journal of River Engineering*, 1(1), 6. <https://doi.org/10.5281/zenodo.18264>
- Patel, D. P., Ramirez, J. A., Srivastava, P. K., Bray, M., & Han, D. (2017). Assessment of flood inundation mapping of Surat city by coupled 1D/2D hydrodynamic modelling: A case application of the new HEC-RAS 5. *Natural Hazards*, 89, 93–130.
- Pathan, A. I., & Agnihotri, P. G. (2020). Application of new HEC-RAS version 5 1D hydrodynamic flood modelling with special reference through geospatial techniques: A case of River Purna of Navsari, Gujarat, India. *Modelling Earth Systems and Environment*, 7, 1133–1144. <https://doi.org/10.1007/s40808-020-00961-0>
- Pender, G., & Neelz, S. (2011). Flood inundation modelling to support flood risk management. In G. Pender & H. Faulkner (Eds.), *Flood risk science and management* (pp. 324–257). Blackwell Publishing Ltd.
- Pramanik, N., Panda, R. K., & Sen, D. (2010). One dimensional hydrodynamic modelling of river flow using DEX extracted river cross-sections. *Water Resources Management*, 24, 835–852. <https://doi.org/10.1007/s11269-009-9474-6>
- Pramanik, S. K., & Rao, K. N. (1952). Hydrometeorology of the Damodar catchment. *Indian Journal of Meteorology & Geophysics*, 3(2), 429–431.
- Raghunath, H. M. (2006). *Hydrology – Principles, analysis and design*. New Age International Publishers.
- Rajbanshi, J. (2015). Rainfall distribution and its spatial and temporal variability over Damodar Basin under climate change scenario (1901–2002). *IOSR Journal of Environmental Sciences, Toxicology and Food Technology*, 9(9), 95–104.
- Rakhecha, P. R., & Singh, V. P. (2017). Enveloping curves for the highest floods of river basins in India. *International Journal of Hydrology*, 1(3), 79–84.
- Rana, V. K., & Suryanarayana, T. M. V. (2021). Estimation of flood influencing characteristics of watershed and their impact on flooding in data-scare region. *Annals of GIS*, 27(4), 397–418.
- Rao, A. R., & Hamed, K. H. (2000). *Flood frequency analysis*. CRC Press, Boca Raton. <https://doi.org/10.1201/9780429128813>
- Rao, A. R., & Hamed, K. H. (2019). *Flood frequency analysis*. CRC Press.

- Roy, P. K., & Mazumdar, A. (2007). Study on hydrology and drought in the flood region of Damodar River Basin. *Journal of Geological Society of India*, 69(5), 1011–1019.
- Rudra, K. (2018). *Rivers of the Ganga-Brahmaputra-Meghna Delta*. Springer Nature.
- Saha, S. K. (1979). River-basin planning in the Damodar Valley of India. *Geographical Review*, 69(3), 273–287.
- Sahoo, B., & Bhaskaran, P. K. (2016). Assessment on historical cyclone tracks in the Bay of Bengal, east coast of India. *International Journal of Climatology*, 36(1), 95–109.
- Saikia, P., & Konwar, K. (2020). Analysis of changes in groundwater levels using Mann-Kendall and Sen's slope estimator in Kamrup (M) District, Assam. In R. Sarkar (Ed.), *Geography in the 21st century: Emerging issues and the way forward* (pp. 357–368). Namya Press.
- Sanyal, J. (2017). Uncertainty in levee heights and its effect on the spatial pattern of flood hazard in a floodplain. *Hydrological Sciences*, 62(9), 1483–1498. <https://doi.org/10.1080/02626667.2017.1334887>
- Sanyal, J., Carbonneau, P., & Densmore, A. L. (2013). Hydraulic routing of extreme floods in a large ungauged river and the estimation of associated uncertainties: A case study of the Damodar River, India. *Natural Hazards*, 66, 1153–1171. <https://doi.org/10.1007/s11069-012-0540-7>
- Sanyal, J., Densmore, A. L., & Carbonneau, P. (2014a). Analysing the effect of land use – Land cover changes at sub-catchment levels on downstream flood peaks: A semi-distributed modelling approach with sparse data. *Catena*, 118, 28–40. <https://doi.org/10.1016/j.catena.2014.01.015>
- Sanyal, J., Carbonneau, P., & Densmore, A. L. (2014b). Low-cost inundation modelling of the reach scale with sparse data in the lower Damodar River Basin, India. *Hydrological Sciences*, 59(12), 2086–2102. <https://doi.org/10.1080/02626667.2014.884718>
- Sarhadi, A., Soltani, S., & Modares, R. (2012). Probabilistic flood inundation mapping of ungauged rivers: Linking GIS techniques and frequency analysis. *Journal of Hydrology*, 458–459, 68–86.
- Sen, P. K. (1985). The genesis of floods in the Lower Damodar catchment. In P. K. Sen (Ed.), *The concepts and methods in geography* (pp. 71–85). The University of Burdwan.
- ShahiriParsa, A., Noori, M., Heydari, M., & Rashidi, M. (2016). Floodplain zoning simulation by using HEC-RAS and CCHE2D models in the Sungai Maka River. *Air, Soil and Water Research*, 9, 55–62.
- Sharma, P., Patil, P., & Eslamain, S. (2022). Flood forecasting time series or flood frequency analysis? In S. Eslamain & F. Eslamain (Eds.), *Flood handbook analysis and modelling* (pp. 131–150). CRC Press.
- Singh, R. K., Villuri, V. G. K., & Pasupuleti, S. (2019). Assessment of parameters and preparation of hydrodynamic model for lower Dmaodar Basin using geomatic techniques. *Masum*, 70(4), 815–824.
- Singh, R. K., Villuri, V. G. K., Pasupuleti, S., & Nune, R. (2020). Hydrodynamic modeling for identifying flood vulnerability zones in lower Damodar River of eastern India. *Ain Shams Engineering Journal*, 11(4), 1035–1046. <https://doi.org/10.1016/j.asej.2020.01.011>
- Singh, R. K., Soni, A., Kumar, S., Pasupuleti, S., & Gobind, V. (2021). Zonation of flood prone areas by an integrated framework of a hydrodynamic model and ANN. *Water Supply*, 21(1), 80–97. <https://doi.org/10.2166/ws.2020.252>
- Sinha, B., & Rao, P. R. (1985). A study for optimum utilization of the Damodar water resources. *Sadhana*, 8, 273–290. <https://doi.org/10.1007/BF02811290>
- Sinha, R., Latrubesse, E. M., & Nanson, G. C. (2012). Quaternary fluvial systems of tropics: Major issues and status of research. *Palaeogeography, Palaeoclimatology, Palaeoecology*, 356–357, 1–15.
- Stelling, G. S., & Verway, A. (2005). Numerical flood simulation. In M. G. Anderson (Ed.), *Encyclopaedia of hydrological sciences* (pp. 1–14). Wiley. <https://doi.org/10.1002/0470848944.hsa025a>
- Subramanya, K. (2013). *Engineering hydrology*. Tata McGraw Hill.

- Surwase, T., Manjusree, P., Sachin Prakash, S., & Kuntla, S. (2020). Development of algorithms for evaluating performance of flood simulation models with satellite-derived flood. *H₂Open Journal*, 3(1), 222–235. <https://doi.org/10.2166/h2oj.2020.117>
- Tate, E. C., & Maidment, D. R. (1999). *Floodplain mapping using HEC-RAS and ArcView GIS*. University of Texas.
- Teng, J., Jakeman, A. J., Vaze, J., Croke, B. F. W., Dutta, D., & Kim, S. (2017). Flood inundation modelling: A review of methods, recent advances and uncertainty analysis. *Environmental Modelling and Software*, 90, 201–216.
- United States Army Corps of Engineers. (2020). *HEC-RAS River Analysis System. HEC-RAS hydraulic reference manual version 6.0 Beta*. US Army Corps of Engineers Hydrologic Engineering Center. <https://www.hec.usace.army.mil/confluence/rasdocs/ras1dtechref/latest>
- Verma, R. K., Murthy, S., & Tiwary, R. K. (2015). Assessment of environmental flows for various sub-watersheds of Damodar River Basin using different hydrological methods. *International Journal of Waste Resources*, 5(4). <https://doi.org/10.4172/2252-5211.1000182>
- Verma, R. K., Murthy, S., Verma, S., & Misgra, S. K. (2017). Design flow duration curves of environmental flows estimation in Damodar River Basin, India. *Applied Water Sciences*, 7, 1283–1293.
- Viji, R., Prasanna, P. R., & Ilangovan, R. (2015). GIS based SCS – CN method for estimating runoff in Kundahpalam Watershed, Nilgries District, Tamilnadu. *Earth Sciences Research Journal*, 19(1), 59–64.
- Vogel, R. M., & Castellarin, A. (2017). Risk, reliability, and return periods and hydrologic design. In V. P. Singh (Ed.), *Handbook of applied hydrology* (pp. 78-1–78-10). McGraw-Hill Education.
- Ward, R. C. (1978). *Floods: A geographical perspective*. Macmillan.
- Zade, M., Ray, S. S., Dutta, S., & Panigrahy, S. (2005). Analysis of runoff pattern for all major basins of India derived using remote sensing data. *Current Science*, 88(8), 1301–1305.